

**V.I. Il'icev Pacific Oceanological Institute
Far East Branch, Academy of Sciences of Russia**

**Results of Acoustic Studies Within and Adjacent to the
Piltun-Astokh License Area**

**1 to 6 August 2001
and
17 to 24 September 2001**

Sakhalin, Russian Federation

**S.V. Borisov
A.V. Gritsenko
A.N. Rutenko
A.V. Hodzevich**

**Prepared for
Exxon Neftegas Limited
&
Sakhalin Energy Investment Company,**

**Yuzhno-Sakhalinsk, Sakhalin,
Russian Federation**

31 July 2002

Table of Contents

LIST OF FIGURES.....	II
LIST OF TABLES	IV
EXECUTIVE SUMMARY	V
1 INTRODUCTION.....	1
1.1 Objectives of the acoustic program	2
1.2 Acoustic recording and processing equipment	3
1.3 Terminology and algorithms used in the report	4
1.4 Units	5
2 DESCRIPTION OF ACOUSTIC DATA RECORDED.....	6
3 ANALYSIS OF THE ACOUSTIC DATA FROM STATION T.6	8
3.1 Measurements of acoustic background near Piltun lighthouse - summer 2001	8
4 ANALYSIS OF AMBIENT NOISE DATA AND ACOUSTIC DATA FROM THE MOLIKPAQ AND <i>IRBIS</i>	17
4.1 Analysis of noise generated by the vessel <i>Irbis</i> on the Sakhalin continental shelf	17
4.2 Acoustic characterization of equipment on the Molikpaq platform	26
5 ANALYSIS OF THE ANTHROPOGENIC ACOUSTIC FIELD FROM THE MOLIKPAQ COMPLEX	31
5.1 Characteristics of the acoustic field between Molikpaq and Piltun	31
6 CONCLUSIONS.....	47
7 FUTURE PLANS.....	48
8 ACKNOWLEDGEMENTS	49
9 AUTHORS	49
10 BIBLIOGRAPHY	50
APPENDIX A - METHODOLOGY FOR NORMALIZING AND ANALYZING THE ACOUSTIC DATA	51

LIST OF FIGURES

- Figure 1.1 - Map of the study area showing the locations of sonobuoys (T.6, B.1 ... B. 5), and potential sources of anthropogenic noise (Molikpaq, *Okha*, and *Irbis*).
- Figure 3.1 - Sonograms of ambient noise recorded at location $\tau.6$ during the night of 1 August 2001.
- Figure 3.2 - Relative spectra characterizing the temporal variation in ambient noise within the 10-2500 Hz frequency band. The data was recorded at location $\tau.6$ during the night of 1 August 2001.
- Figure 3.3 - Sonograms of acoustic noise recorded at location $\tau.6$ during the day on 2 August 2001. Acoustic pulses generated from 16:00h - 18:30h were recorded with significant non-linear distortion due to the sonobuoy being overdriven.
- Figure 3.4 - Sonograms of acoustic noise recorded at location $\tau.6$ during the night of 4-5 August 2001.
- Figure 3.5 - Sonograms of acoustic noise recorded at location $\tau.6$ during the night of 5-6 August 2001.
- Figure 4.1 - Sonograms $G(f,t)$ and spectra $G(f)$ of acoustic noise synchronously recorded at locations B.3 and B.4 while the *Irbis* was steaming toward location B.2.
- Figure 4.2 - Sonograms $G(f,t)$ and spectra $G(f)$ of acoustic noise synchronously recorded at locations B.4, B.3 and B.2 while the *Irbis* was steaming toward location B.1.
- Figure 4.3 - Sonograms $G(f,t)$ and spectra $G(f)$ of acoustic noise synchronously recorded at locations B.4, B.3, B.2 and B.1 while the *Irbis* was steaming toward location B.5.
- Figure 4.4 - Sonograms $G(f,t)$ and spectra $G(f)$ of acoustic noise synchronously recorded at locations B.4, B.2, B1 and B.5 while the *Irbis* was steaming from shore towards its anchorage. *Irbis* cast anchor at 21:10h.
- Figure 4.5 - Sonograms $G(f,t)$ and spectra $G(f)$ of acoustic noise synchronously recorded at locations B.4, B.2, B1 and B.5 while the *Irbis* was steaming from shore towards its anchorage. *Irbis* cast anchor at 21:10h.
- Figure 4.6 - Sonograms $G(f,t)$ and spectra $G(f)$ of acoustic background synchronously recorded at locations B.4, B.3, B.2, B1 and B.5 during the night of 18 September 2001.

Figure 4.7 - Sonograms $G(f,t)$ and spectra $G(f)$ of acoustic background synchronously recorded at locations B.4, B.3, B.2, B.1 and B.5 during the night of 18 September 2001.

Figure 4.8 - relative spectra $G(f)$ of acoustic noises recorded in the ballast chamber of the Molikpaq at 09:30h on 18 September 2001.

Figure 4.9 - Relative spectra $G(f)$ of acoustic noises recorded on the deck above the ballast chamber of the Molikpaq at 10:00h on 18 September 2001.

Figure 5.1 - Sonograms $G(f,t)$ of acoustic noise synchronously recorded at locations B.4, B.3, B.2, B.1 and B.5 during 18 September 2001 (day).

Figure 5.2 - Relative spectra $E(f)$ of acoustic noise synchronously recorded at locations B.4, B.3, B.2, B.1 and B.5 while the signal was recorded at Molikpaq.

Figure 5.3 - Spectra $G(f)$ of acoustic noise synchronously recorded at locations B.4, B.3, B.2, B.1 and B.5 during 18 September 2001.

Figure 5.4 - Spectra $G(f)$ of tonal acoustic noise synchronously recorded at locations B.4, B.3, B.2, B.1 and B.5 during 18 September 2001.

Figure 5.5 - Sonograms $G(f,t)$ of acoustic noise synchronously recorded at locations B.4, B.3, B.2, B.1 and B.5 during the night of 19 September 2001.

Figure 5.6 - Sonograms $G(f,t)$ of acoustic noise synchronously recorded at locations B.2, B.1 and B.5 during 21-22 September 2001.

Figure 5.7 - Spectra $G(f)$ of acoustic noise synchronously recorded at locations B.2, B.1 and B.5 at 15:50h, 17:05h, 18:05h and 18:55h on 21 September 2001.

Figure 5.8 - Spectra $G(f)$ of acoustic noise synchronously recorded at locations B.2, B.1 and B.5 at 20:10h, 21:30h and 21:40h on 21 September 2001.

Figure 5.9 - Spectra $G(f)$ of acoustic noise synchronously recorded at locations B.2, B.1 and B.5 at 00:20h, 02:00h, 02:15h and 03:20h on 22 September 2001.

Figure 5.10 - Sonograms $G(f,t)$ of acoustic noise synchronously recorded at locations B.2, B.1 and B.5 during 22 September 2001 (day).

Figure 5.11 - Spectra $G(f)$ of acoustic noise synchronously recorded at locations B.2, B.1 and B.5 at 18:56h, 20:16h, 21:34h and 21:46h on 22 September 2001.

Figure 5.12 - Sonograms $G(f,t)$ of acoustic noise synchronously recorded at locations B.2, B.1 and B.5 during 23 September 2001 (day).

LIST OF TABLES

Table 2.1 - Time date and location of monitoring sonobuoys.

Executive Summary

Environmental Impact Assessments (EIA) conducted prior to the development of the oil and gas resources off the NE Sakhalin coast determined that the key marine environmental issue is protection of western gray whales (*Eschrichtius robustus*) that spend most of the ice-free season feeding off the NE Sakhalin coast. These whales are listed as endangered in the Russian Red Book (Red Book of the Russian Federation, 2001) and critically endangered by the International Union for the Conservation of Nature (IUCN) (Hilton-Taylor 2000). Photo identification reports have indicated that some individuals have been emaciated during the past few years.

Gray whale sightings from 1999 and 2000 indicated that feeding gray whales were predominantly localized shoreward of the 20 m water depth contour, in the area near the mouth of Piltun Bay and northward along the NE Sakhalin coast.

The SEER panel has requested that the Odoptu Gray Whale Monitoring Program investigate the cumulative impact of the planned development on this population with specific focus on the impact of low frequency sound. In early August 2001 acoustic measurements were made near the mouth of Piltun Bay. In late September 2001 acoustic measurements were also made on and near the Molikpaq platform, and between the Molikpaq platform and the mouth of Piltun Bay. Further measurements of ambient noise and measurements of anthropogenic noise generated by construction and production activities are planned for 2002 and beyond.

The acoustic measurements showed that the Molikpaq platform and Vityaz oil complex have pronounced tonal and narrowband acoustic components, some below 30 Hz, with spectral levels 10-15 dB higher than the level of the broadband noise. The most intensive acoustic noise sources at frequencies below 1 kHz were found to be support vessels. Anthropogenic acoustic signals generated by stationary and moving sources are consistently recorded in the gray whale feeding area off the mouth of Piltun Bay. The spectral levels of these tonal and narrowband signals (at frequencies below 500 Hz) were ~80-90 dB re 1 $\mu\text{Pa}^2/\text{Hz}$.

1 Introduction

The acoustic program conducted on the NE shelf of Sakhalin Island in 2001 had two main objectives. The first was to evaluate and monitor the acoustic transmission from the Odoptu seismic survey, the second to study both temporal and spatial variations in the amplitude and frequency characteristics of anthropogenic acoustic noise near the mouth of Piltun Bay¹. The first objective was discussed in a separate report [Borisov et. al. 2002], the second objective is the subject of this report. Acoustic measurements were made near the mouth of Piltun Bay in early August and on the continental shelf of the Okhotsk Sea, between Molikpaq and the mouth of Piltun Bay in mid-September. The dominant source of anthropogenic acoustic noise in this area is the equipment operating on the Molikpaq platform and the oil storage vessel *Okha*, as well as transient noise generated by the vessels supporting the oil-production complex Vityaz, especially steaming or anchored tankers. The seismic vessel *Nordic Explorer* also acquired seismic data in the area north of 52° 57' N during the August-September time frame [Borisov et. al., 2002]. The outboard motors from zodiacs operating near the major concentrations of gray whales constitute a further source of transient noise in the area. Zodiacs have been used in this way by the group of scientists based at Piltun lighthouse for a number of years.

Earlier studies [Cummings et al. 1968] showed that gray whales can produce signals at frequencies as low as 15 Hz; however, the majority of signals produced by gray whales consist of a set of impulses with their acoustic energy concentrated in the frequency band from 300 to 800 Hz (Richardson et al. 1995). In order to evaluate the possible impact of anthropogenic noise on the feeding gray whales, it was necessary to determine the amplitude and spectral content of these noises and the characteristics of sound propagation to the mouth of Piltun Bay. This is an area where the gray whales are concentrated, and feed in water depths of ~6-12 m (Sobolevsky et al. 1999, 2000, Yazvenko et al. 2002).

Figure 1.1 is a map of the study area showing the locations where ambient acoustic noise measurements were made by sonobuoys (τ.6, B1, ... B5). The map also shows the location of the Molikpaq platform and oil storage vessel *Okha*, which are connected by an underwater pipeline (all are potential sources of noise). The map also shows the acoustic

¹ The mouth of Piltun bay is one of the summer feeding grounds for the Korean-Okhotsk (western) gray whale.

transect Molikpaq-Piltun along which acoustic measurements were made. The mouth of

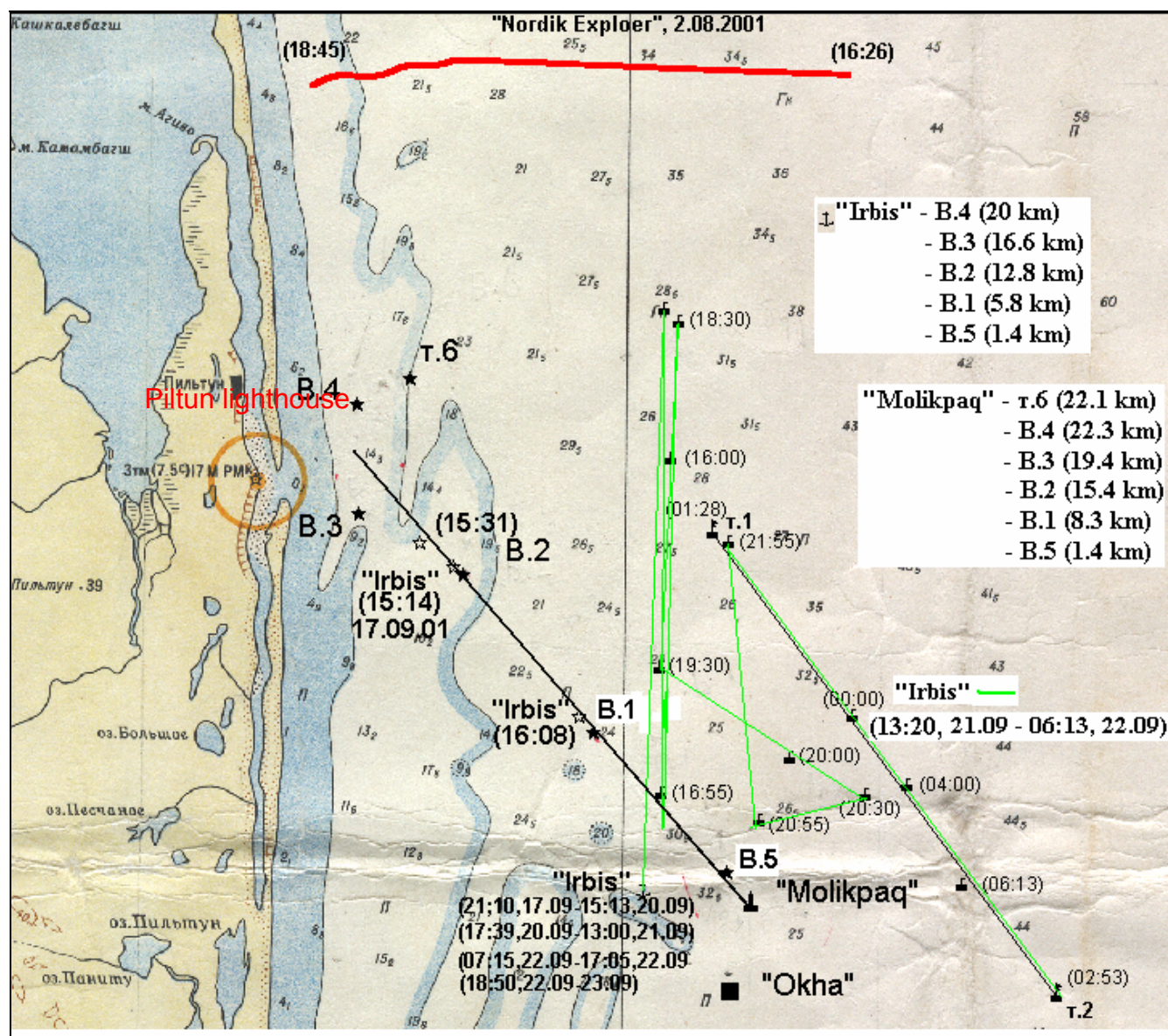


Figure 1.1 - Map of the study area showing the locations of sonobuoys (T.6, B.1 ... B. 5), and potential sources of anthropogenic noise (Molikpaq, Okha, and Irbis).

Piltun Bay is approximately opposite Piltun lighthouse, which is marked by the orange circle².

1.1 Objectives of the acoustic program

The objective of this element of the acoustic program was to deploy sonobuoys to

² Due to the movement of the spit, the map in Figure 1.1 is inaccurate and location B.3 is across from the entrance to Piltun Bay

determine the spectral characteristics of noise generated by the Vityaz production complex and the acoustic propagation between the complex and the main gray whale feeding area.

1. Using sonobuoys located within the gray whale feeding area, conduct acoustic background measurements under a range of weather conditions and during a variety of operations on Molikpaq that could be expected to generate acoustic noise.
2. Measure anthropogenic noise generated by the Molikpaq on the Molikpaq.
3. Study the temporal and spatial variation of anthropogenic noise; determine the amplitude and spectral content of noise generated by the main stationary and moving noise sources.

1.2 Acoustic recording and processing equipment

Individually deployed autonomous sonobuoys were used to measure acoustic signals in the frequency band from 10 Hz to 5 kHz and transmit them to a shore station via radio. The acoustic signals are derived from a hydrophone mounted in a pyramid shaped wire frame on the bottom³. Two types of hydrophones were used; standard disc hydrophones of type PR-1 (ПР-1) and cylindrical hydrophones of type PR-2 (ПР-2). A frequency dependent gain correction in the amplifier-corrector amplifies the low frequency components of the signal, compensating for the lower low frequency response of the pre-amplifier. This equalization of amplitudes across the frequency band optimizes the use of the dynamic range of the radio receivers and transmitters. Analog data received at the shore station was converted to digital data by an analog to digital converter (ADC) and accumulated in a digital format on the hard drive of a laptop computer⁴. The system was capable of filtering, digitizing, visualizing and accumulating data from up to eight independent sonobuoys. A detailed description of the characteristics and calibration of the acoustic recording equipment is provided elsewhere [Borisov et. al. 2002].

The received level (RL) of acoustic noise depends on the hydrophone deployment depth and the distance between the potential noise source and the sonobuoy. The gain coefficients of a sonobuoy must be set to maximize the dynamic range of the radio-telemetry channel. The closer the sonobuoy is deployed to the Molikpaq, the higher the level of acoustic noise and the lower the gain (and thus sensitivity) of the sonobuoy.

³ The hydrophone converts acoustic pressure to voltage.

⁴ Data were stored on laptop hard drives in 650Mb folders, facilitating the backup of data to CD's.

Therefore, sonobuoys deployed further away from Molikpaq (in the shallow part of the study area) (T.6, B.4, and B.3) have higher gain coefficients than those deployed closer.

Sonobuoys were deployed from a zodiac or the support vessel *Irbis*. Signals were received on the *Irbis* or at Piltun lighthouse. The signals from the five sonobuoys (Figure 1.1, locations B.1 to B.5) were received at Piltun lighthouse using multi-element radio antennae⁵. This allowed synchronous reception and storage of acoustic data.

1.3 Terminology and algorithms used in the report

Ambient and anthropogenic noise recorded by the sonobuoys was written to disc in microPascals (μPa)⁶. Acoustic spectra in decibels will be used to describe the variation in acoustic power as a function of frequency. In this report sound pressure energy density spectra ($\mu\text{Pa}^2/\text{Hz}$)⁷ or power density spectra ($\mu\text{Pa}^2/(\text{s Hz})$)⁸ will be used when spectral data are plotted.

The **Spectral level** of noise relates to the level of acoustic power in a 1 Hz band. This term is only applied to sounds with continuous frequency spectra⁹. These spectra are often averaged over 10-300 one-second windows¹⁰ to improve the statistical stability of the ambient noise data¹¹.

The sonograms are plots of frequency vs. time, the scales generally run from ~40 to ~105 dB re 1 $\mu\text{Pa}^2/\text{Hz}$.

The acoustic measurements made by sonobuoys yield a synchronous series of spatially discrete data. This data set will allow the temporal, spatial and spectral¹² characteristics of the acoustic field to be evaluated. Noise (signal) produced by a moving vessel has a

⁵ Standard AX-700

⁶ The data was scaled (after incorporating hydrophone sensitivity and system gain) to convert the data to standard units of pressure (measured through an omni-directional hydrophone) in real time.

⁷ Energy and power spectra are scaled to 1 Hz whatever the analysis length.

⁸ Acoustic intensity.

⁹ A continuous frequency spectrum is a spectrum with signal present at all sampled frequencies.

¹⁰ Average of 10 or 300 1 second spectral realizations.

¹¹ Spectral averaging will lead to the cancellation of zero mean errors in instrument noise leading to an improvement in the ambient noise/instrument noise level at low ambient noise levels.

¹² The spectral characteristics of the acoustic field were analyzed within the frequency range of the recording system.

continuous spectrum with discrete tonal components. Equipment operating on the Molikpaq (gas generators, compressors, pumps, etc.) is also a source of continuous tonal and broadband acoustic noise. This could include infrasonic (<20 Hz) noise.

A detailed description of the methodology used for normalizing and analyzing both the amplitude and spectral data is given in Appendix A.

1.4 Units

During the course of this report a number of different unit notations have been used. This is due to differences in standard notation between different disciplines and nationalities.

The following are equivalent units using the different standard nomenclatures:

$$1 \text{ mkPa} = 1 \text{ } \mu\text{Pa}$$

$$1 \text{ mkV} = 1 \text{ } \mu\text{V}$$

It should also be remembered that:

$$1 \text{ atm} \cong 1 \text{ bar} = 0.1 \text{ MPa} = 10^{11} \text{ } \mu\text{Pa}$$

For spectral density plots:

Although the units for power spectral density are $\mu\text{Pa}^2/(\text{s Hz})$, $\mu\text{Pa}^2/\text{s/Hz}$ or μPa^2 , it is common usage to define the units for power spectral density as $\mu\text{Pa}^2/\text{Hz}$ or $\mu\text{Pa}/\sqrt{\text{Hz}}$.

2 Description of Acoustic Data Recorded

Table 2.1 gives the coordinates of the sonobuoys used in the study (τ.6, B1, ... B5) and plotted in Figure 1.1, the start and completion of acoustic recording with each sonobuoy as well as the deployment depth of their hydrophones.

№	Date/Time		Ch #	Sonobuoy	Latitude	Longitude	Depth (m)
	Begin	Finish					
1	01.08.01 23:55	06.08.01 14:23	1	τ.6	52°52'54.1"N	143°23'19.5"E	20
2	17.09.01 14:20	21.09.01 08:00	1	B.4	52°52'24"N	143°21'09"E	10
3	17.09.01 15:00	21.09.01 08:00	2	B.3	52°50'18"N	143°21'50"E	11
4	17.09.01 15:34	24.09.01 08:42	3	B.2	52°49'10"N	143°25'01"E	14
5	17.09.01 16:14	24.09.01 08:42	4	B.1	52°46'10"N	143°29'00"E	20
6	17.09.01 17:20	24.09.01 08:42	5	B.5	52°43'30"N	143°33'06"E	24

Table 2.1 - Time date and location of monitoring sonobuoys.

In early August, acoustic measurements were made using a sonobuoy located at point τ.6. During this time frame acoustic experiments to calibrate the buffer zone were conducted by the seismic vessel *Nordic Explorer* north of 52°57' N. The *Nordic Explorer* acquired seismic data while steaming parallel and perpendicular to the coast; each of these calibration experiments was conducted for approximately two to three hours during daylight [Borisov et. al., 2002]. The tanker *Primorye* arrived in the Molikpaq area during these experiments (i.e. on 4 August), but due to poor weather could only approach the floating complex *Okha* on the afternoon of 6 August.

On 17 September, five sonobuoys were deployed from the vessel *Irbis* at locations B.1 to B.5 (Figure 1.1). Radio signals from these five buoys were received at Piltun lighthouse. This allowed signals from all five sonobuoys to be simultaneously recorded on one laptop.

On 18 September, two scientists with recording equipment transferred from the *Irbis* to the Molikpaq and conducted acoustic measurements on the platform. The measurements were made inside the ballast room, which is located below the water line at the base of Molikpaq. Measurements of the vibration of the main deck of Molikpaq were also conducted with the hydrophones lying in a puddle of water.

A log was kept of all vessels working in the Molikpaq area for the duration of the September acoustic study. The name of any vessel present, a description of its activity, and its coordinates were recorded. On 22 September, at 14:00h the tanker *Primorye* moored at the floating complex *Okha* and at 16:45h began off-loading oil. Oil off-loading was completed at 03:00h on 23 September and at 08:20h the *Primorye* left the *Okha* complex. During the off-loading of the oil, the vessel *Smit Sakhalin* was used to provide stable orientation of the chain of two tankers at the floating pier that connects the *Okha* with the Molikpaq and its engines were constantly running.

During the period of this study measurements of the acoustic field were conducted at several locations. These acoustic measurements provide quantitative estimates of the levels of ambient and anthropogenic noise generated by vessels and equipment supporting the operation of the Vityaz oil production complex. This data allowed us to estimate the amplitude levels of the seismic pulses generated by the seismic vessel *Nordic Explorer* and the support vessels *Rubin* and *Atlas* during the Odoptu 3D seismic survey [Borisov et. al. 2002]. Simultaneous measurements of the noise levels at five separate locations between Molikpaq and Piltun enable the analysis of the spectral, spatial and temporal characteristics of the acoustic field in the area.

3 Analysis of the Acoustic Data from station $\tau.6$

This section describes the results of spectral analysis of ambient noise measured in the gray whale feeding area near Piltun Bay. The measurements were made under varying weather and sea conditions and reflect both a quiet acoustic environment and an acoustic environment characterized by anthropogenic noise.

3.1 Measurements of acoustic background near Piltun lighthouse - summer 2001

Acoustic measurements were made from 1-6 August using one sonobuoy located at point $\tau.6$ (Figure 1.1)¹³. Figures 3.1 and 3.2 show sonograms¹⁴ $G(f,t)$ and the spectral estimates $G(f)$ computed from measurements of ambient noise made during the night of 1 August, 2001. Different values of power spectral density $G(f,t)$ (dB re 1 mkPa^2/Hz) on Figure 3.1 are indicated by different colors. The spectral density plots allow quantitative estimation of the spectral-temporal structure of the acoustic field at point $\tau.6$ and the analysis and identification of stationary and moving sources of tonal and broadband noise. The sonograms $G(f,t)$ cover a broad (0-1500 Hz) and a narrow (0-500 Hz) band of frequencies to aid in the visual analysis of the data. The acoustic measurements were recorded over frequencies from 10 - 5000 Hz. Ambient noise levels are known to be less at frequencies above 3 kHz than at low frequencies, also the dynamic range of the sonobuoys was limited to ~ 35 dB. The sonograms were therefore plotted over the frequency range in which the level of the acoustic signals was within the dynamic range of the buoy¹⁵.

Figure 3.1 represents the spectral-temporal structure of the acoustic field at point $\tau.6$. The ambient noise is dominated by stationary sources of low frequency tonal and narrowband noise. The sonograms $G(f,t)$ and spectra $G(f)$ in Figures 3.2 and 3.3 show the amplitude and frequency of a real anthropogenic signal. This anthropogenic signal could be a vessel at sea¹⁶ or equipment at or near Piltun lighthouse. Figure 3.2 shows that the amplitude of the ambient noise spectra¹⁷ decreases linearly with increased frequency at frequencies above 250 Hz. This frequency dependent decrease is approximately -0.01dB/Hz .

¹³ The sonobuoy at location $\tau.6$ was lost in a storm and was not cross-calibrated. The data can therefore not be used to calculate absolute amplitudes and only a relative amplitude analysis can be undertaken.

¹⁴ A sonogram is a plot showing the variation in acoustic level with frequency and time.

¹⁵ The dynamic range is confirmed by the frequency-dependent temporal variability of the signals.

¹⁶ A three bladed propeller would have a frequency signature of approximately 38 Hz.

¹⁷ These 2-minute spectral density estimates $G(f)$ are averages of 120 1-second spectral realizations.

G(f,t), T.6, 1.08.2001y.

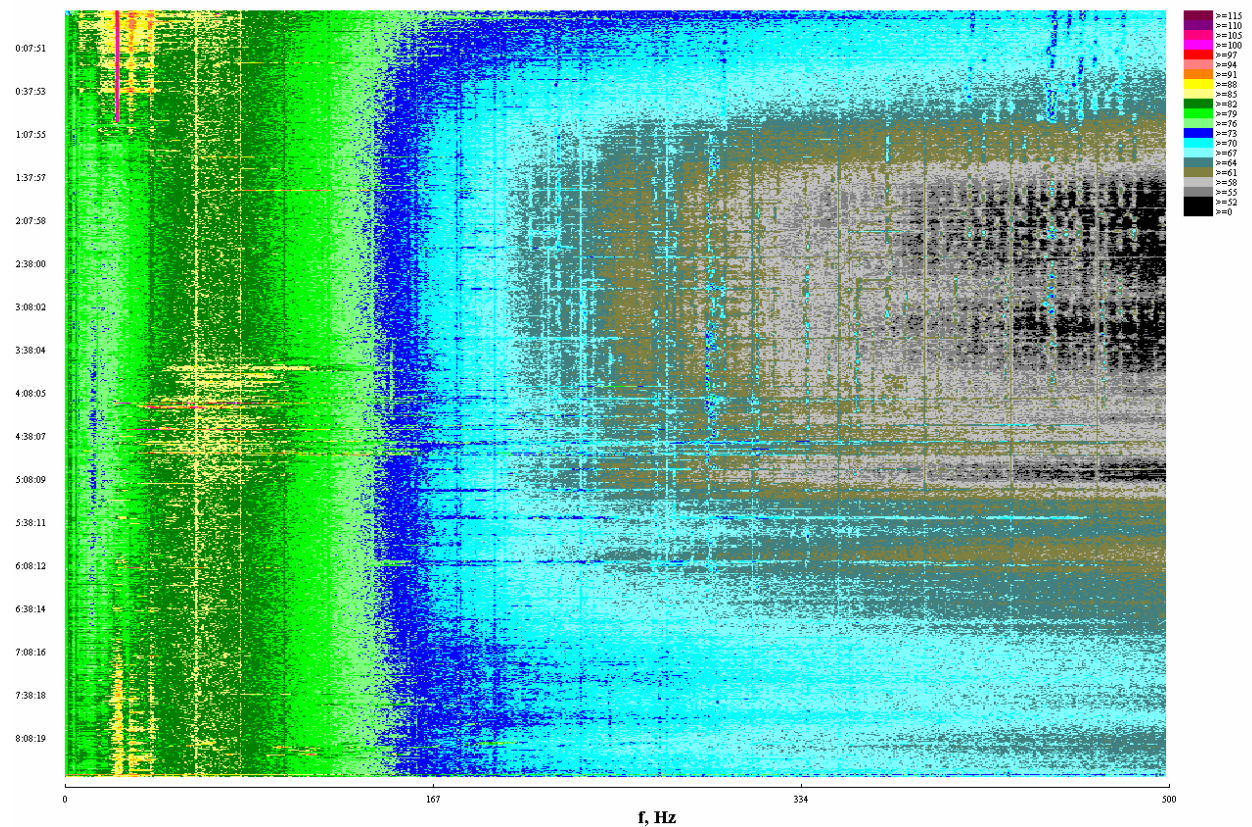
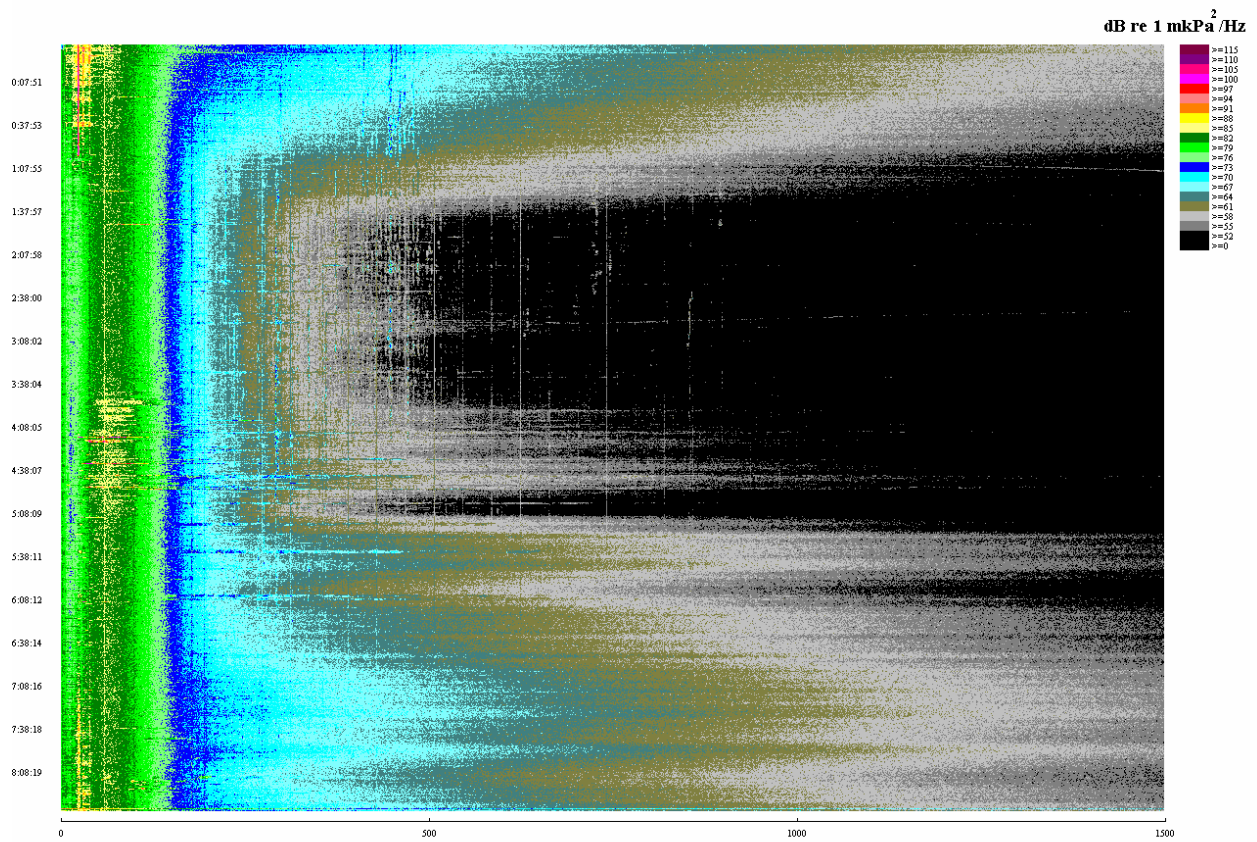


Figure 3.1 - Sonograms of ambient noise recorded at location T.6 during the night of 1 August 2001.

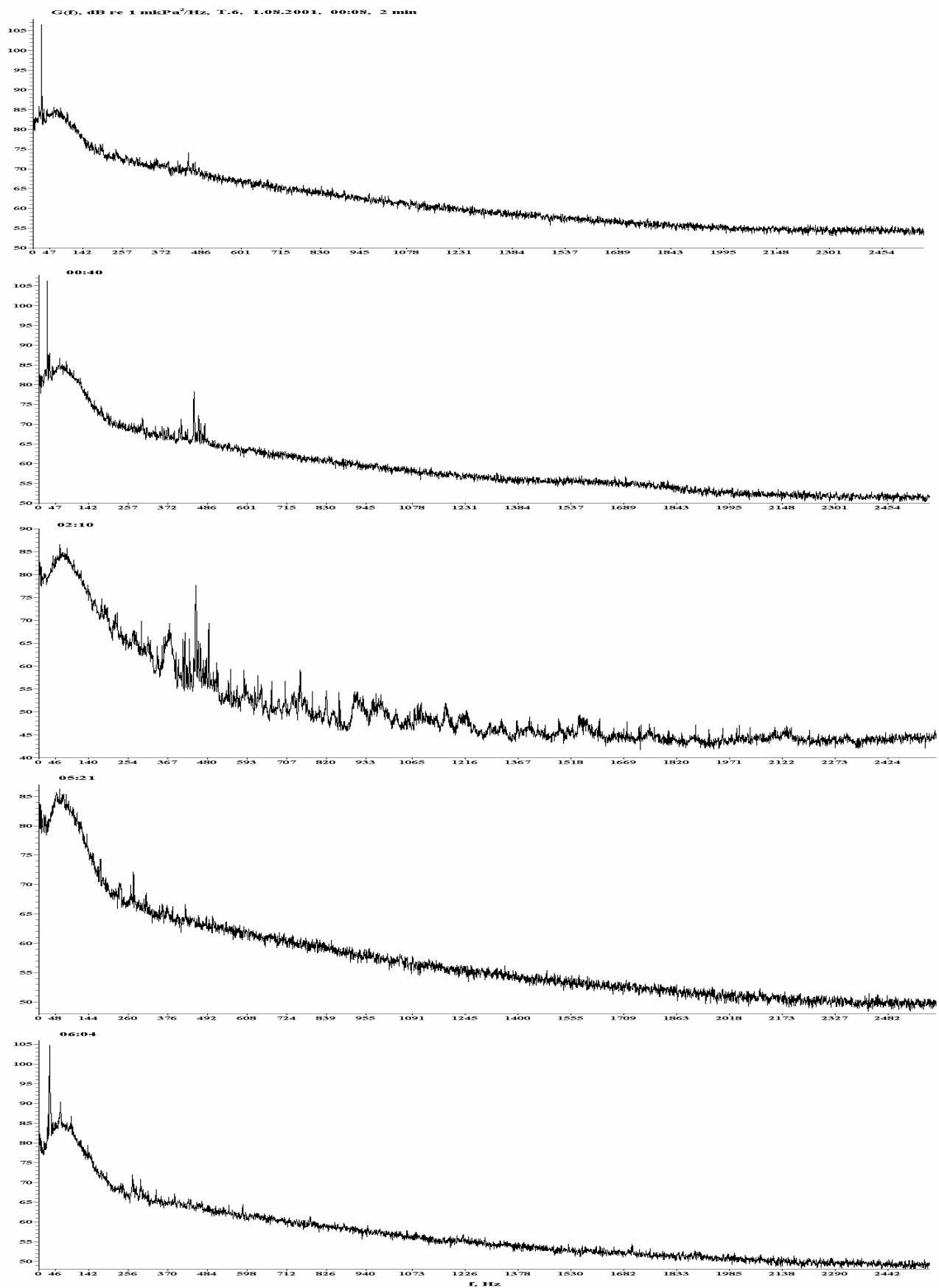


Figure 3.2 - Relative spectra characterizing the temporal variation in ambient noise within the 10-2500 Hz frequency band. The data was recorded at location T.6 during the night of 1 August 2001.

At frequencies of 50-200 Hz a decrease in spectral density of approximately -0.1 dB/Hz is observed. For frequencies between 0-50 Hz the values of $G(f)$ increase. The anthropogenic noise has a pronounced spectral peak at frequencies of 20-30 Hz (Figure 3.2)¹⁸.

Figure 3.3 is a sonogram of the acoustic background recorded at location $\tau.6$ during 2 August 2001 (daytime). On this day an acoustic calibration experiment to determine the buffer zone for the Odoptu seismic survey was conducted in the southern part of the Odoptu program area. The seismic vessel *Nordic Explorer* steamed perpendicular to the coast along the course shown in red on Figure 1 [Borisov et. al. 2002], a southeastern wind caused some white caps (wave height approximately 1 m). The *Nordic Explorer* started ramping up its air gun array at 15:10h and gradually increased the power of the array. After 16:18h the acoustic pulses from the *Nordic Explorer* overloaded the hydrophone¹⁹. At 18:21h the array volume was decreased from 3090 in³ to 100 in³, output from the 100 in³ array did not overload the hydrophone. At the end of the experiment the *Nordic Explorer* sailed south, passing by location $\tau.6$, and then east towards deeper water. Figure 3.3 shows the frequency-spatial interference structure of the acoustic field generated by the moving *Nordic Explorer* from 19:00h-20:30h as it executed this maneuver. At 20:00h the *Nordic Explorer* was at the closest point of approach to location $\tau.6$.

Figure 3.4 is a sonogram of the ambient noise for location $\tau.6$. This corresponds to a time period when there were no moving ships in the vicinity. However, even if a ship is anchored it still emits significant levels of acoustic noise due to moving machinery whose vibrations are transmitted through the submerged section of the hull (the most effective emitter of low frequency sounds in water). The following types of movements can cause vibration:

- Rotation of unbalanced parts of the machine (e.g. eccentric shafts or armatures);
- Vibration of engine fixtures;
- Reciprocating motion of mechanical parts such as pistons in engines;
- Cavitation and turbulence of fluid in pumps, pipelines, valves and condensers; and
- Mechanical resistance in bearings.

¹⁸ The *Rubin* probably generated this anthropogenic noise as they sailed close by the buoy.

¹⁹ This data will not give an accurate spectral measurement as it is overdriven. This buoy had a very high gain coefficient and was significantly more sensitive than the other buoys used in the study. The buoy was located at point $\tau.6$ to record ambient noise data. The acoustic calibration was at the South of the Odoptu area and used the 3090 in³ air gun array that was reduced to 1640 in³ for the seismic survey.

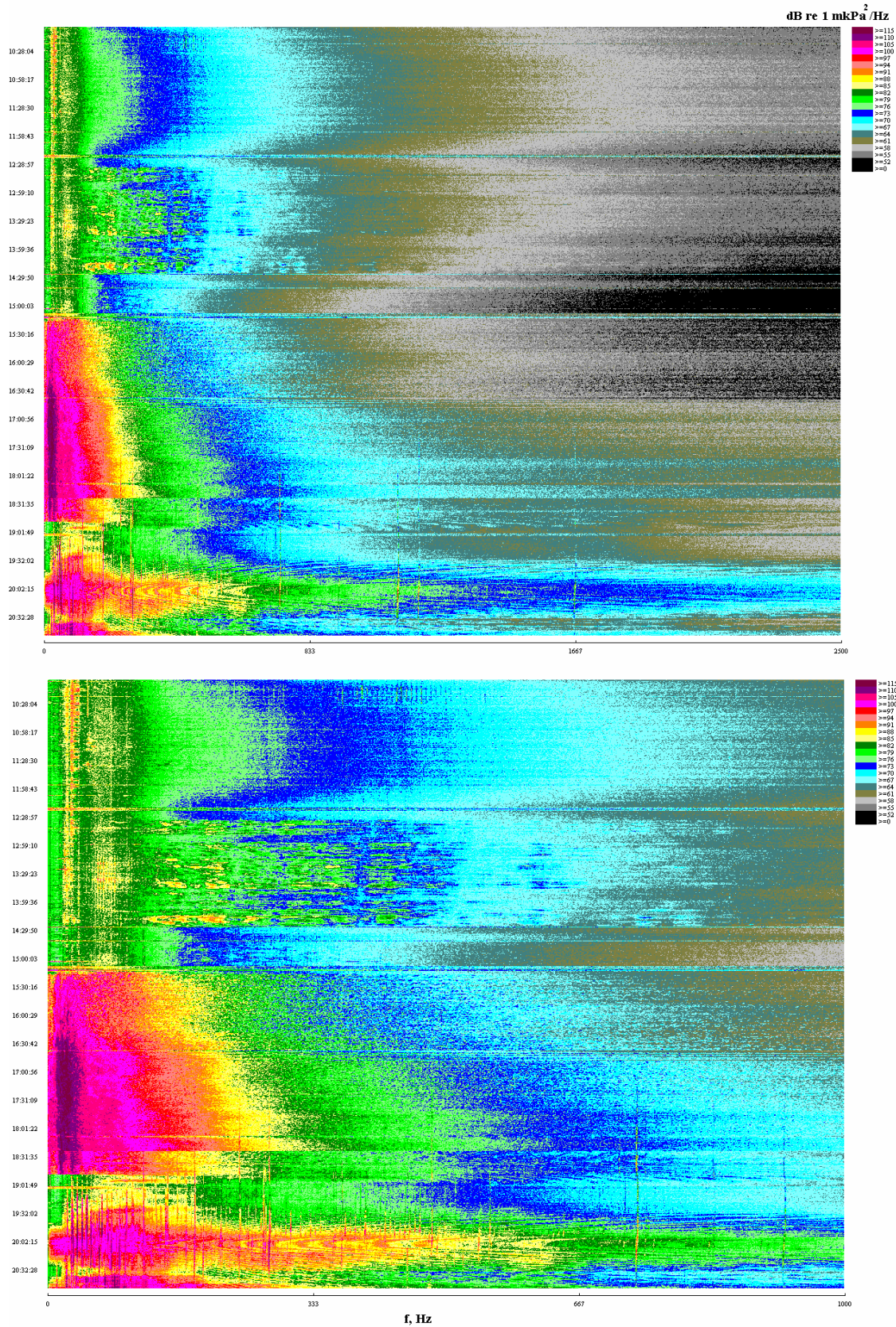


Figure 3.3 - Sonograms of acoustic noise recorded at location T.6 during the day on 2 August 2001. Acoustic pulses generated from 16:00h - 18:30h were recorded with significant non-linear distortion due to the sonobuoy being overdriven.

The first three of the noise sources described above create discrete spectral components, with the predominant components at the rotational frequencies of the process, these discrete components are generated in cases when there are resonance oscillations in the machinery. The last two noise sources create a continuous noise spectrum. The noise spectrum of a piece of equipment is therefore the superimposition of strong discrete components on its continuous noise spectrum.

At 23:00h the weather was clear with a southern wind up to 10 m/s, there was a vessel north of the Molikpaq, and the tanker *Primorye* east of the Molikpaq. The spectral level of the broadband noise does not exceed 64 dB, and low-frequency (20-70 Hz) stable peaks of narrowband signals are clearly seen. Spectral levels of these signals can be 30-35 dB higher than the level of the broadband noise.

The spectral analysis of acoustic signals recorded at location $\tau.6$ during the night of 5-6 August 2001 is shown on Figure 3.5. These will be compared with Figure 3.4, which was recorded at approximately the same time of day one day earlier. At 22:44h on 5 August 2001 there was a storm and it was raining, the tanker *Primorye* was anchored. At 05:50h on 6 August 2001, there was a southeastern wind at 5-7 m/s, and fog with visibility of 400-500 m. Figure 3.5 indicates that at 00:00h on 6 August there was a sharp increase in the amplitude of anthropogenic noises at frequencies between 100-1500 Hz.

The frequency interference pattern indicated in Figure 3.5 shows that the source of the sound was non-stationary and was possibly moving. One possible reason for that change might be the swinging of the *Primorye* around its anchor due to the ebb tide change. After 00:30h the frequency interference pattern stabilized.

In conclusion, during early August 2001, narrowband and tonal noise at frequencies between 12-70 Hz were regularly recorded at location $\tau.6$ (Figure 1.1), this noise varied both in time and in frequency. The level of this narrowband noise was more than 30 dB higher than that of the broadband noise, and is comparable with levels of noise generated by moving ships.

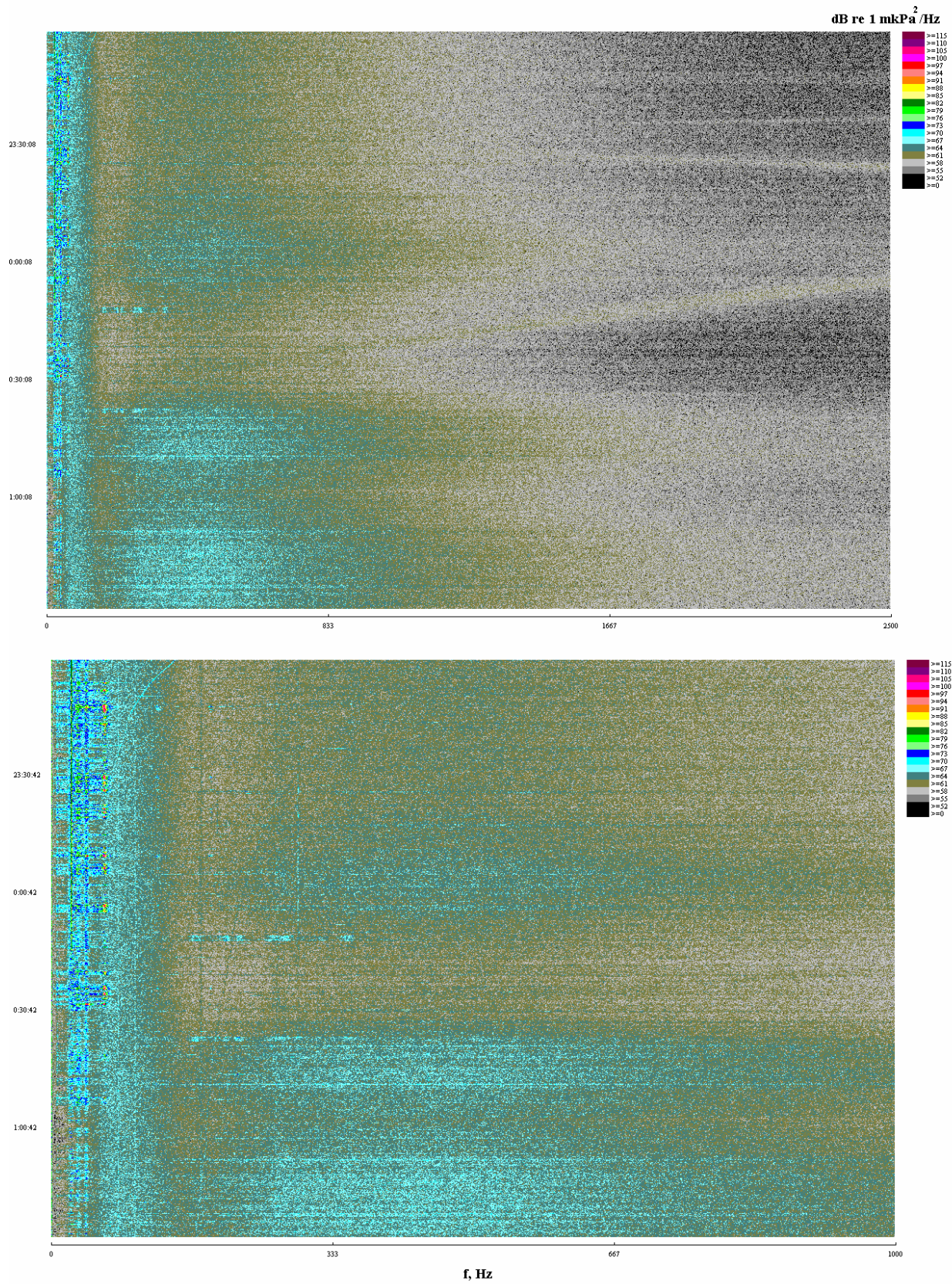


Figure 3.4 - Sonograms of acoustic noise recorded at location T.6 during the night of 4-5 August 2001.

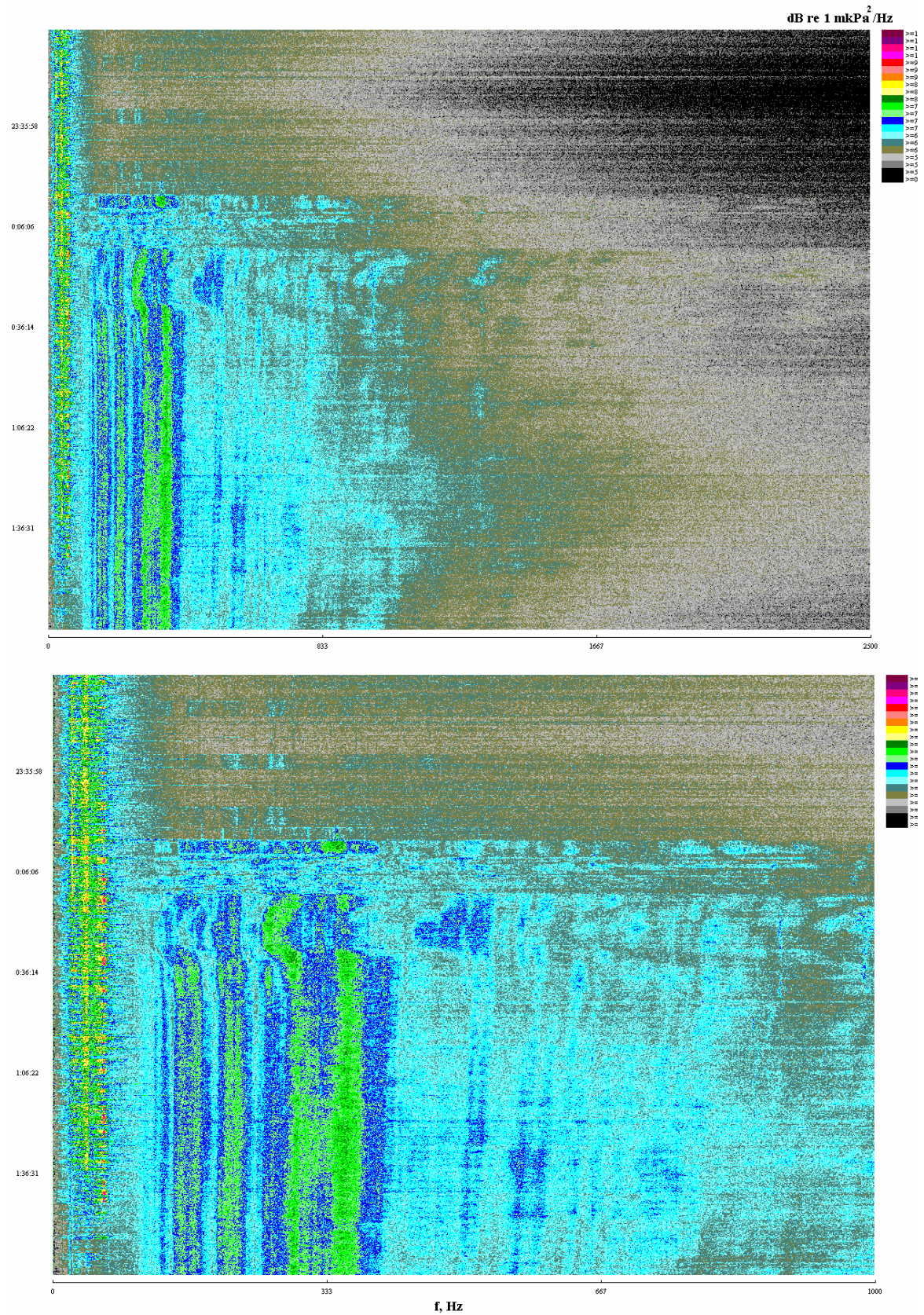


Figure 3.5 - Sonograms of acoustic noise recorded at location T.6 during the night of 5-6 August 2001.

Unfortunately the source of the noise could not be isolated as the acoustic field was only recorded at a single location. It was therefore decided to record the acoustic field using an array of sonobuoys, these were deployed so that the azimuth of the noise could be isolated. These sonobuoys were also cross-calibrated, allowing the absolute spectral value of the noise to be determined.

4 Analysis of Ambient Noise Data and Acoustic Data from the Molikpaq and *Irbis*

This section describes the results of spectral analysis of ambient noise measurements made between the Molikpaq complex and the gray whale feeding area near Piltun Bay. The section also includes the measurement and analysis of acoustic noise generated on or around the Molikpaq and by the *Irbis*.

4.1 Analysis of noise generated by the vessel *Irbis* on the Sakhalin continental shelf

On the morning of 17 August five sonobuoys and recording equipment were transferred to the *Irbis* off the mouth of Piltun Bay. The first sonobuoy was deployed at location B.4 (Figure 1.1) at 14:20h and the second at location B.3 at 15:00h. By 15:14h the *Irbis* was steaming towards location B.2²⁰. At 15:34h the *Irbis* was anchored at location B.2 and a third sonobuoy was deployed at that point. Figure 4.1 shows the spectra of acoustic signals synchronously recorded at locations B.4 and B.3 as the *Irbis* was steaming towards location B.2²¹. Figure 1.1 (open stars) shows the locations of the *Irbis* corresponding to the spectra $G(f)$ (at 15:14h and 15:31h) plotted on Figure 4.1. The curve $G(f)$ at 15:38h (Figure 4.1) shows the acoustic noise generated by the *Irbis* when drifting, but with the engines running. The spectral level of the noise generated by slowly moving or anchored vessels (Figure 4.1) are similar, but the striped part of the noise spectrum is less pronounced when the vessel is anchored. The spectra $G(f)$ are dominated by noise below 100 Hz. The sonobuoy at location B.4 had a disk hydrophone (type PR-1), whereas location B.3 had a cylindrical hydrophone (type PR-2); calibrations of both hydrophones did not reveal any sensitivity anomalies between 10-630 Hz. Therefore, it is likely that the sharp increase in the level of low frequency noise recorded at location B.3 was caused by flow noise generated by the currents and tidal flow near the mouth of the Piltun Bay. Due to the movement of the spit, the map in Figure 1.1 is inaccurate and location B.3 is across from the entrance to Piltun Bay. High levels of very low frequency flow noise may cause non-linear distortions over the entire frequency range; therefore, for quantitative spectral estimates we will preferentially use the data recorded at location B.4.

²⁰ The *Irbis* is powered by one four-blade propeller revolving at approximately 400 rpm

²¹ All the spectra displayed in chapter 4 were derived from data recorded by sonograms that have been cross-calibrated. Absolute pressure levels can therefore be interpreted from this data.

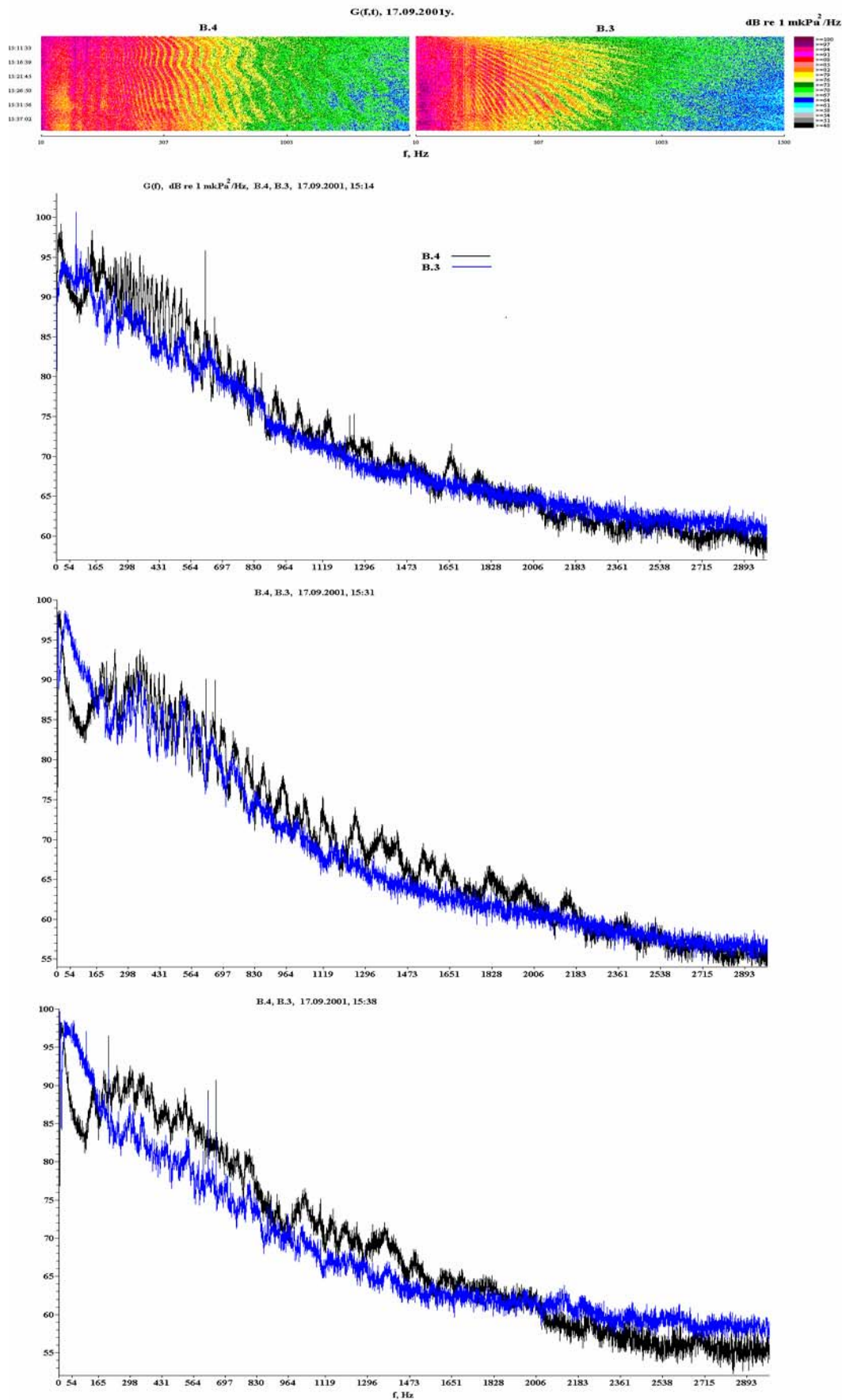


Figure 4.1 - Sonograms $G(f,t)$ and spectra $G(f)$ of acoustic noise synchronously recorded at locations B.3 and B.4 while the Irbis was steaming toward location B.2.

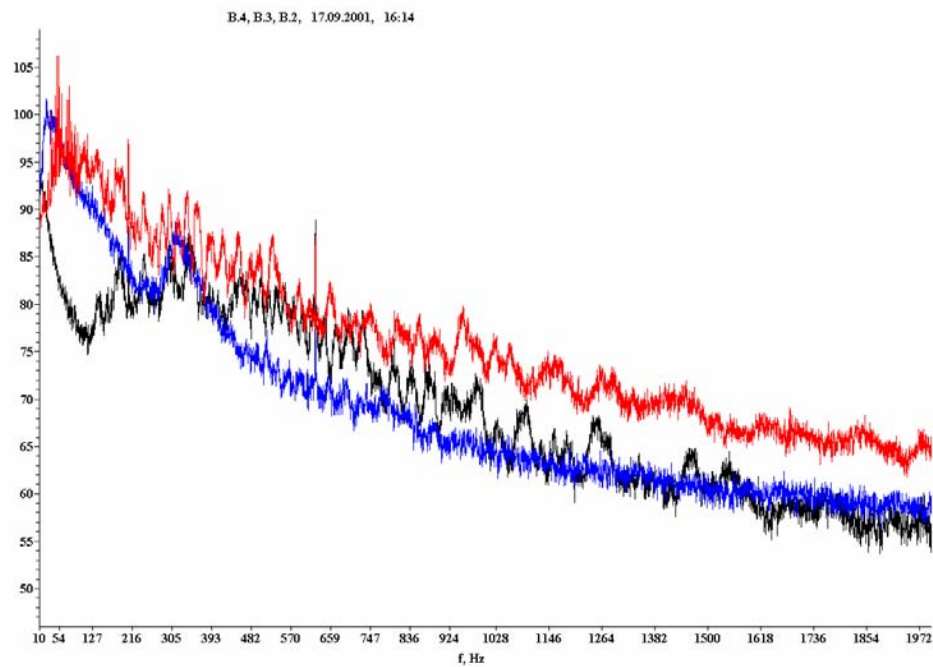
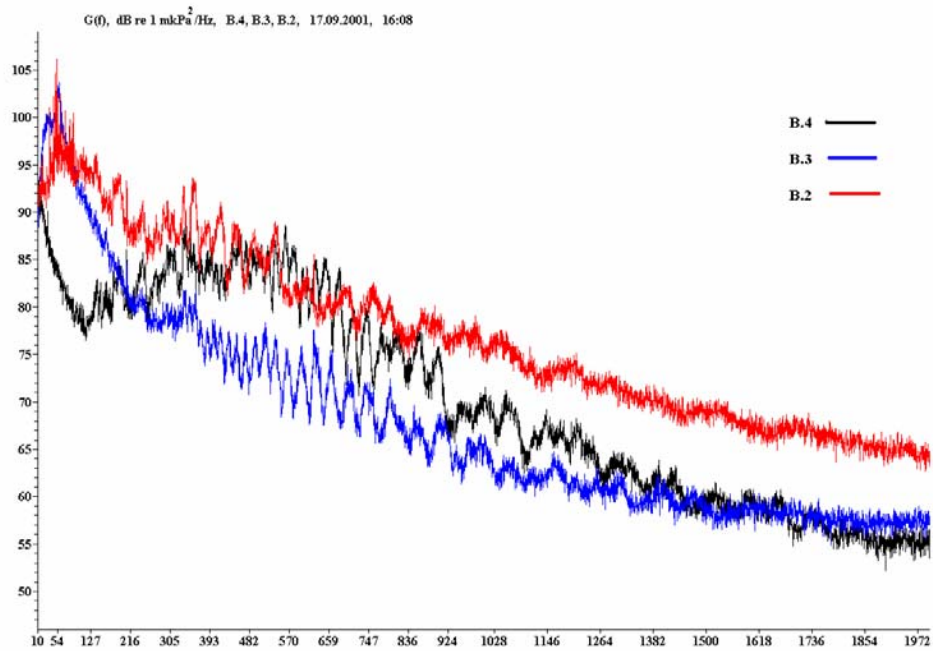
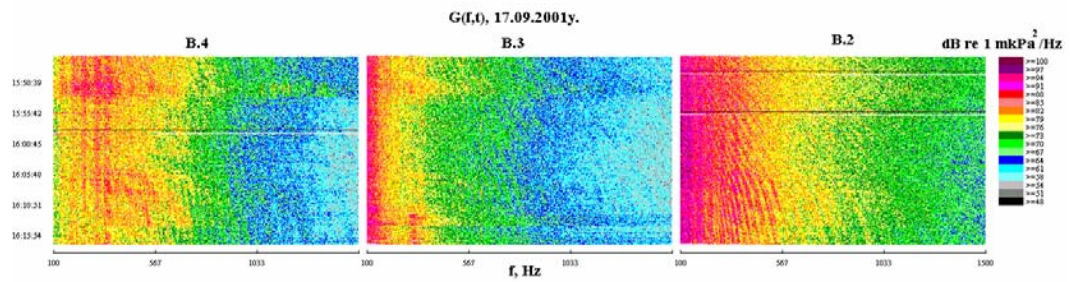


Figure 4.2 - Sonograms $G(f,t)$ and spectra $G(f)$ of acoustic noise synchronously recorded at locations B.4, B.3 and B.2 while the Irbis was steaming toward location B.1.

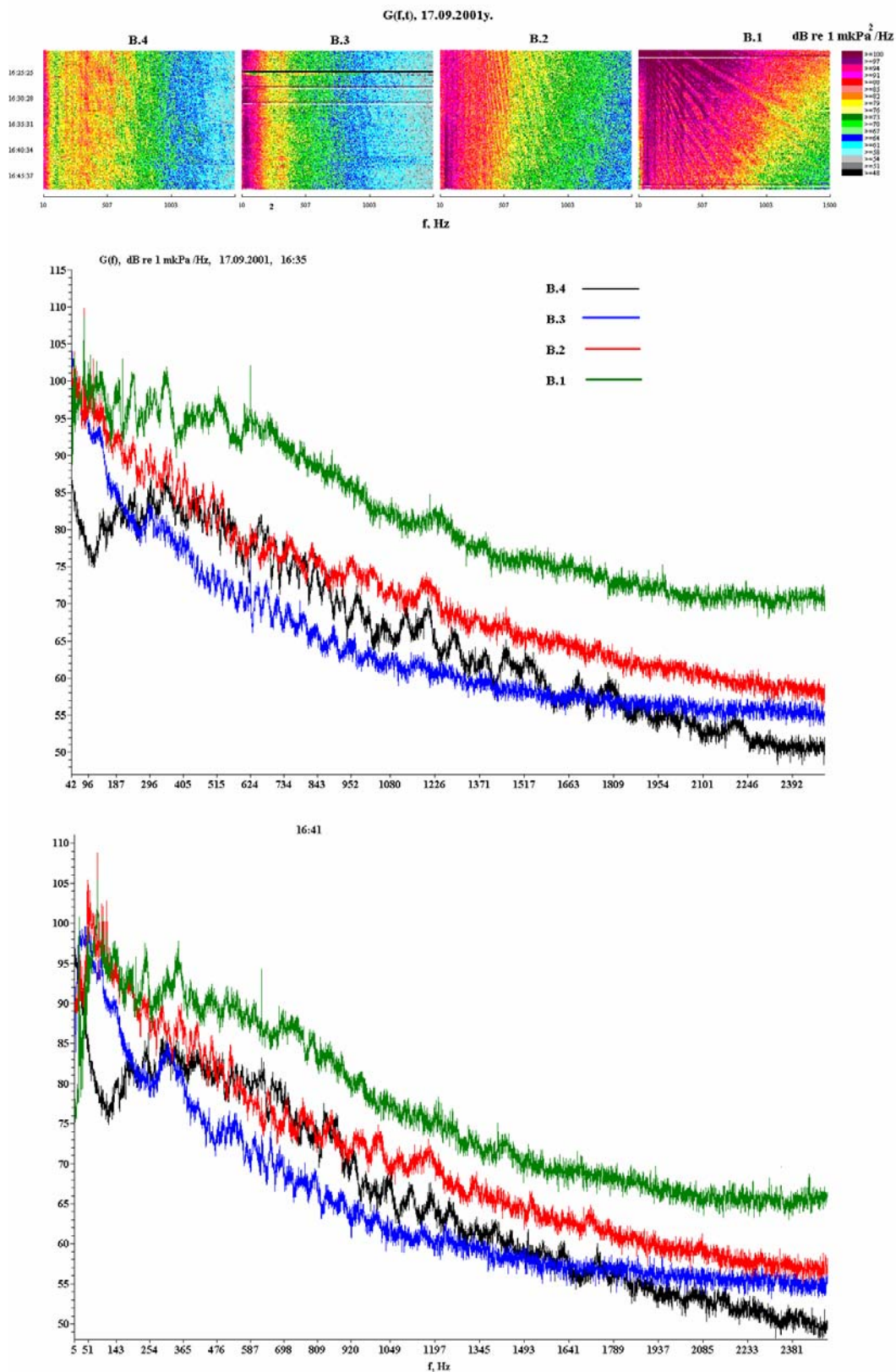


Figure 4.3 - Sonograms $G(f,t)$ and spectra $G(f)$ of acoustic noise synchronously recorded at locations B.4, B.3, B.2 and B.1 while the Irbis was steaming toward location B.5.

Figure 4.2 shows the spectral-spatial interference structure of the acoustic field generated by the *Irbis* while sailing towards location B.1. The spectra $G(f)$ in Figure 4.2 correspond to the position of the *Irbis* shown on Figure 1.1 (at 16:08h). The spectra on Figure 4.3 correspond to synchronous measurements taken at locations B.4, B.3, B.2, and B.1 while the *Irbis* was sailing towards location B.5. These spectra show the characteristic acoustic signature of a vessel sailing in the area between Molikpaq and Piltun.

After the sonobuoy was deployed at location B.5, it was determined that with an AX-700 radio receiver and a directional antenna the signals from the sonobuoy could be reliably received at Piltun lighthouse, it was therefore decided to return the fifth radio receiver to the lighthouse. The *Irbis* therefore returned to Piltun Bay and at 20:00h started moving back towards the Molikpaq, at 20:49h it was within 5 km of the Molikpaq, and by 21:10h was anchored close to the Molikpaq at the location shown on Figure 1.1²². Figures 4.4 and 4.5 show the spectra of acoustic noises synchronously recorded at locations B.4, B.2, B.1, and B.5 between 19:40h and 22:25h. During the same time period, in addition to the *Irbis*, there was another vessel the *Neftegaz-60* working near the Molikpaq (spectrum B.5 on Figure 4.4). At 21:33h the *Smit Sakhalin* was moving from the *Okha* complex towards the Molikpaq. Figure 4.4 shows the spectra $G(f)$ at 20:03h and 20:10h have pronounced tonal and narrowband peaks at frequencies of 690, 1060 and 1340 Hz, these peaks exceed the average background noise by more than 15 dB at location B.5.

Figures 4.6 and 4.7 display the spectral analysis of the acoustic signals synchronously recorded at locations B.1 to B.5 during the night of 18 September 2001. The sonograms $G(f,t)$ of Figure 4.6 show that the noises generated by a vessel moving near the Molikpaq at 02:35h - 03:10h were recorded at all five locations (Spectra $G(f)$ of Figure 4.6 at 02:36h).

²² 52° 43' 00" N; 143° 30' 36" E

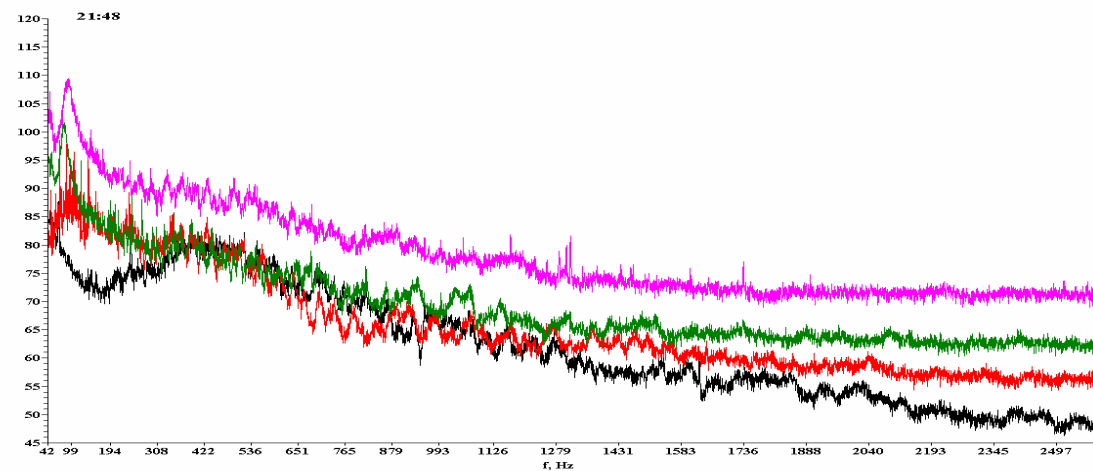
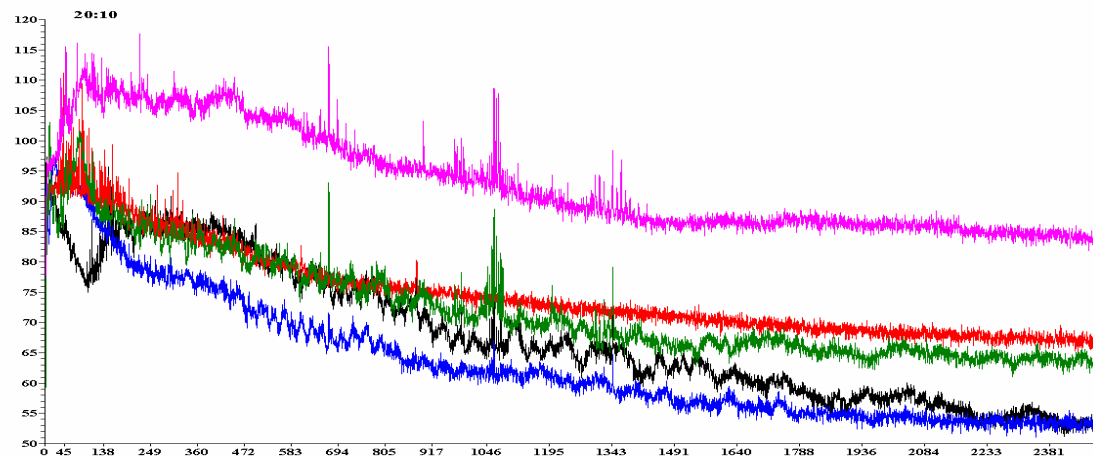
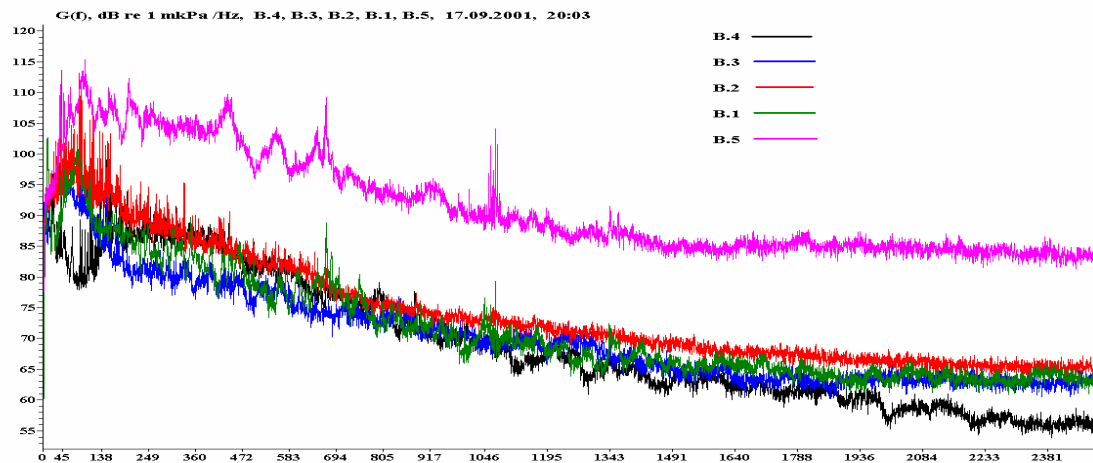
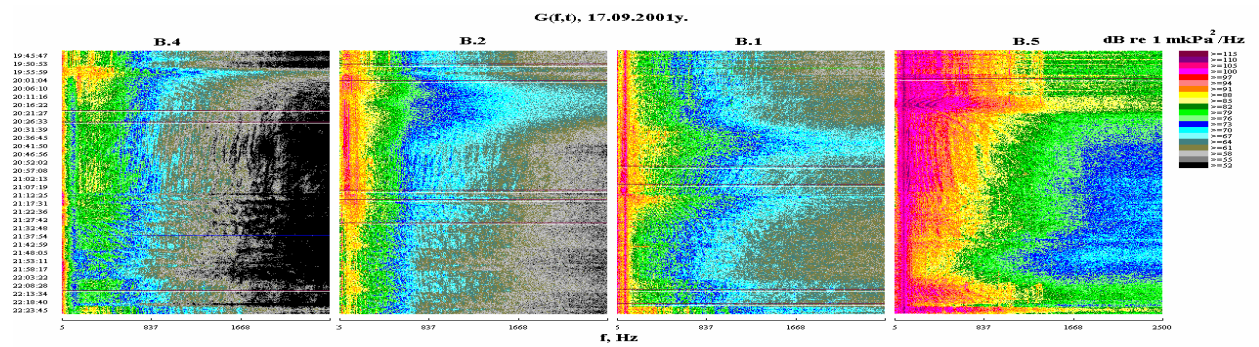


Figure 4.4 - Sonograms $G(f,t)$ and spectra $G(f)$ of acoustic noise synchronously recorded at locations B.4, B.2, B.1 and B.5 while the *Irbis* was steaming from shore towards its anchorage. *Irbis* cast anchor at 21:10h.

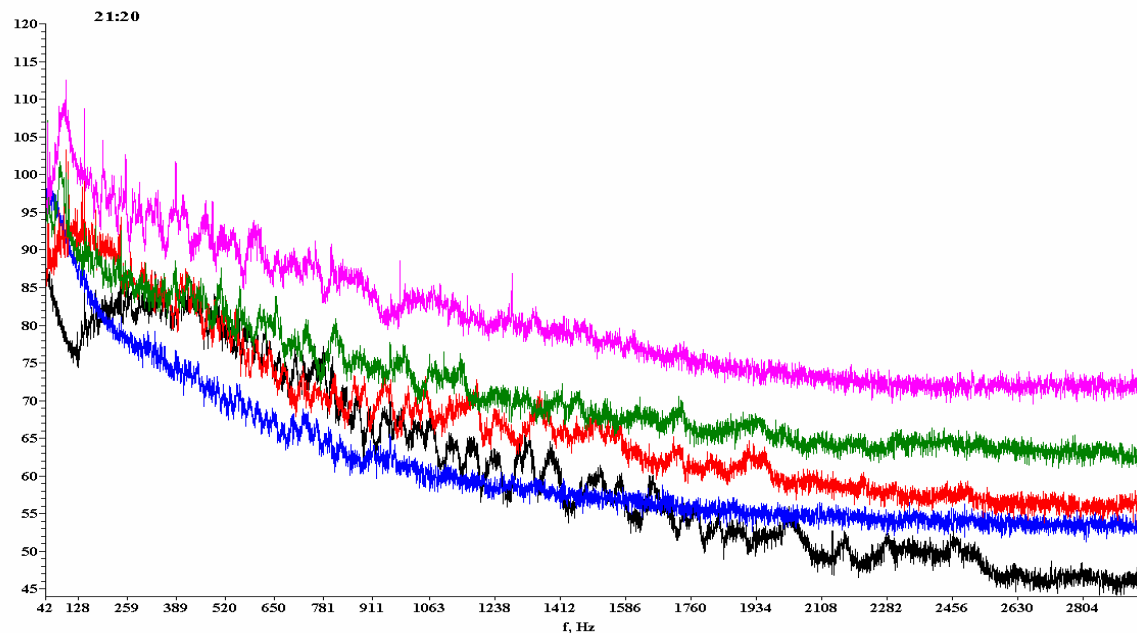
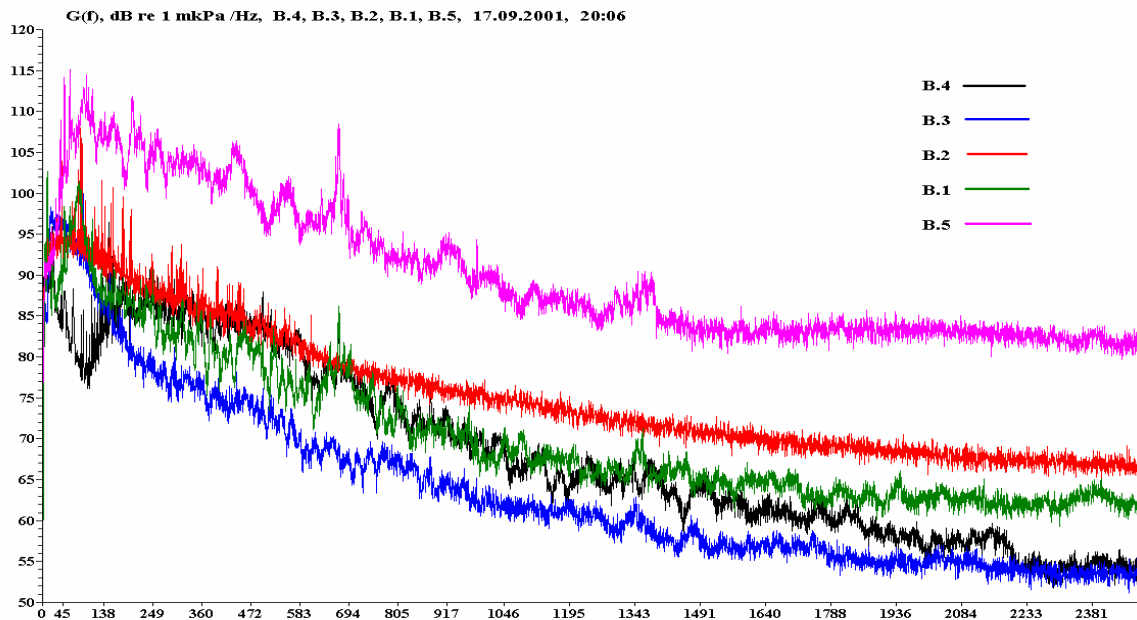
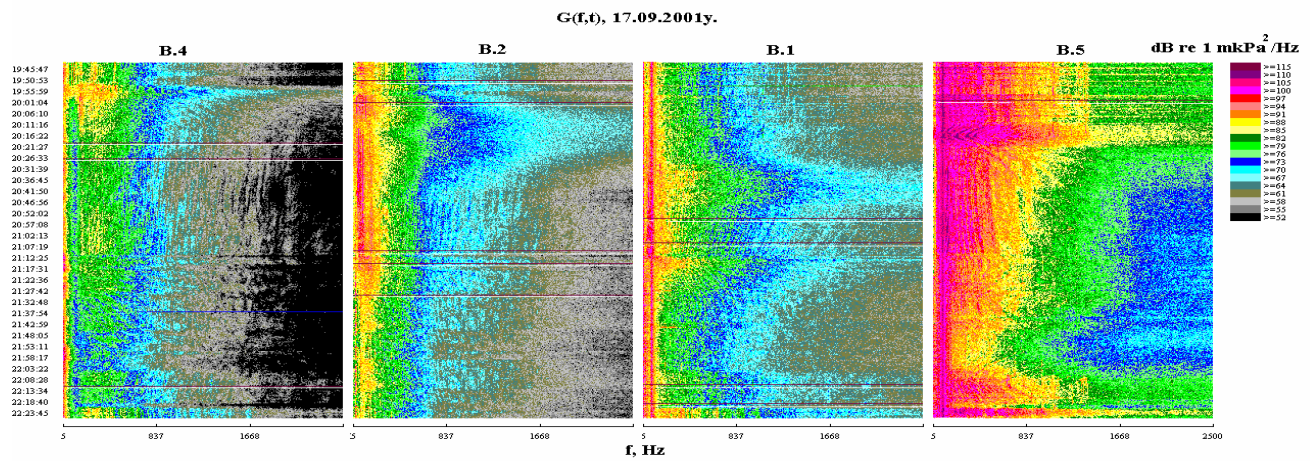


Figure 4.5 - Sonograms $G(f,t)$ and spectra $G(f)$ of acoustic noise synchronously recorded at locations B.4, B.2, B1 and B.5 while the *Irbis* was steaming from shore towards its anchorage. *Irbis* cast anchor at 21:10h.

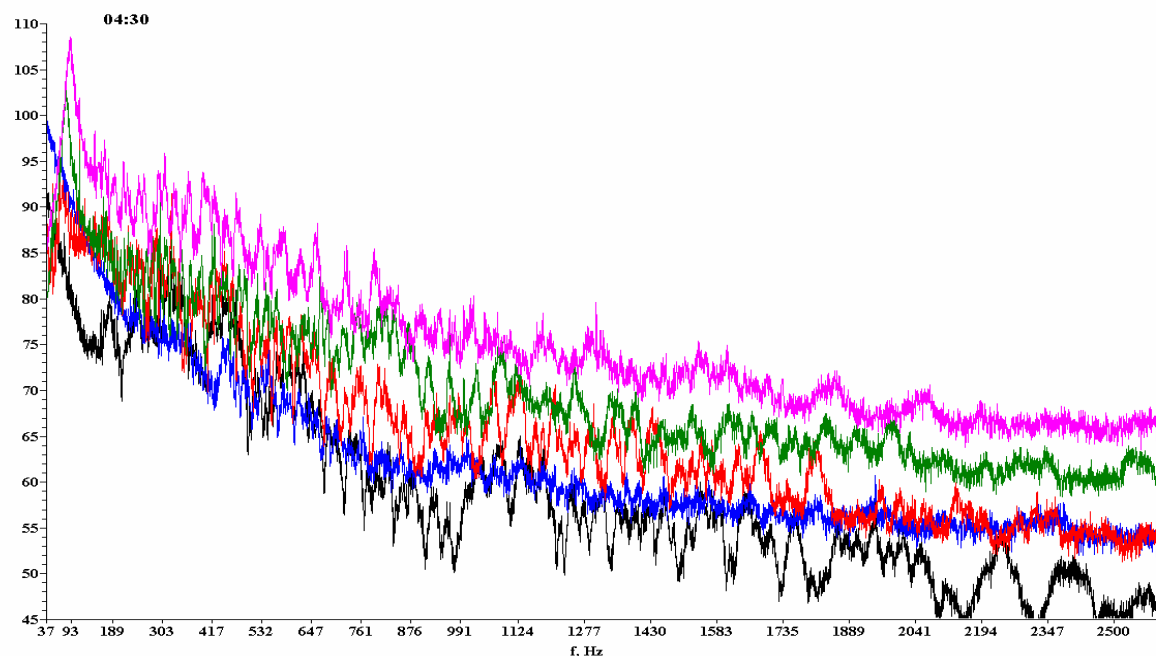
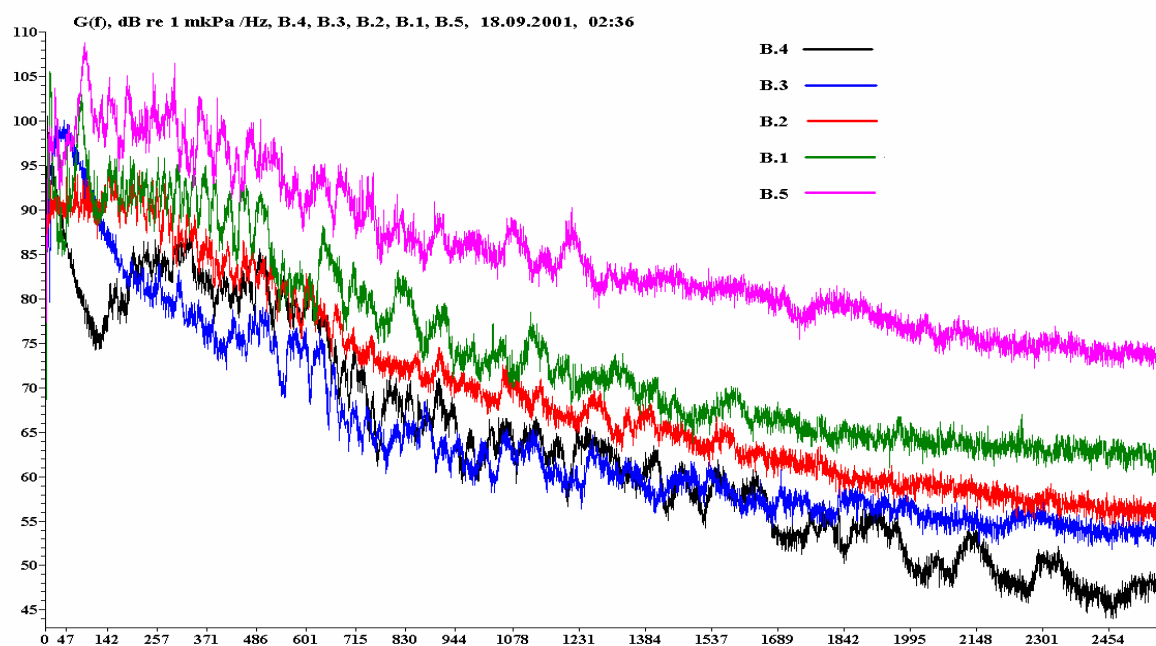
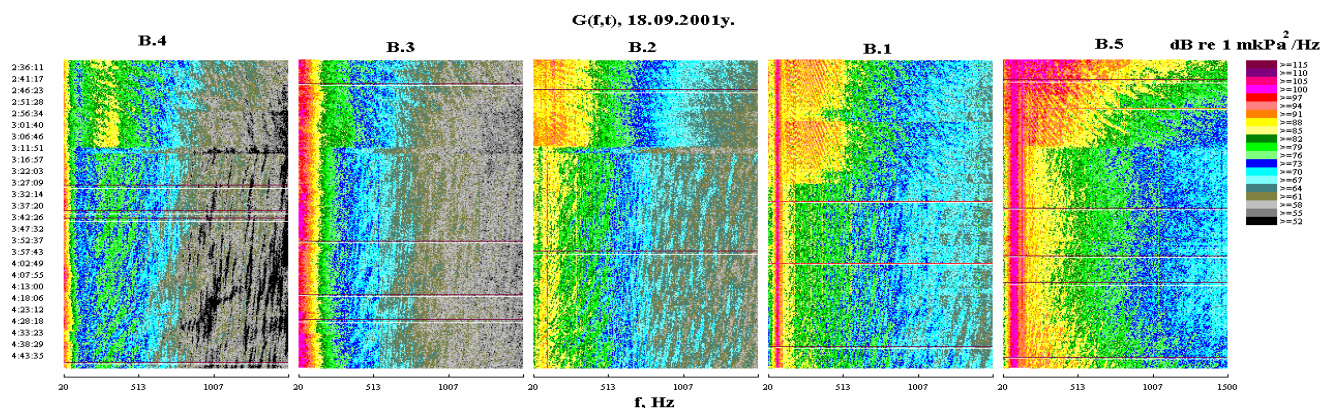


Figure 4.6 - Sonograms $G(f,t)$ and spectra $G(f)$ of acoustic background synchronously recorded at locations B.4, B.3, B.2, B.1 and B.5 during the night of 18 September 2001.

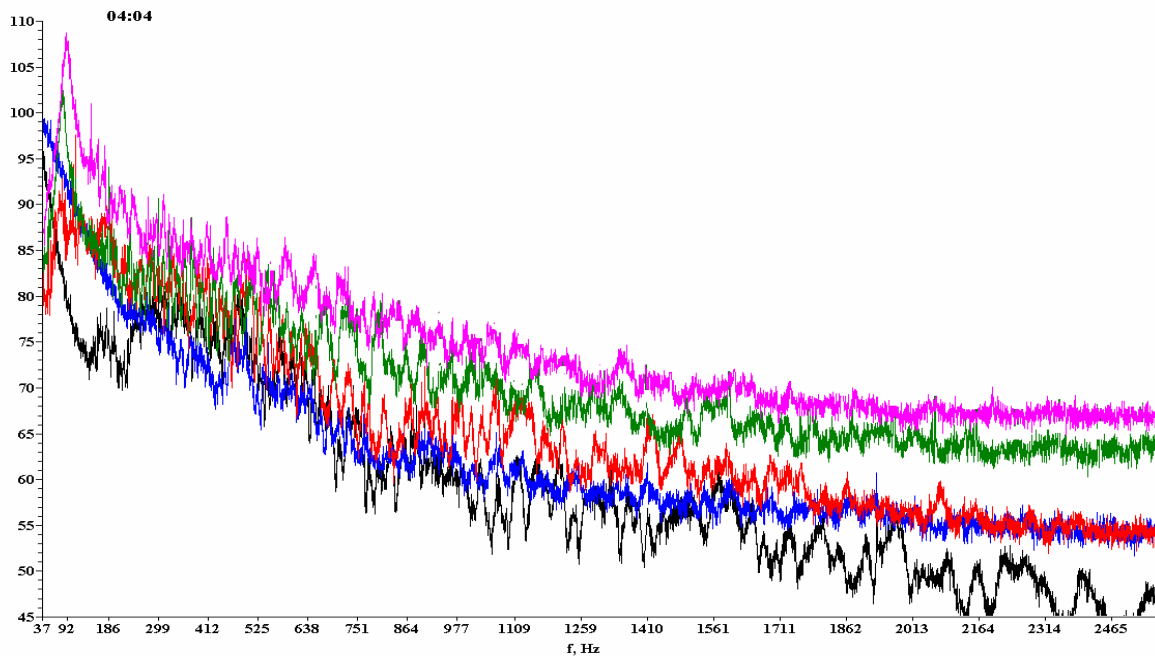
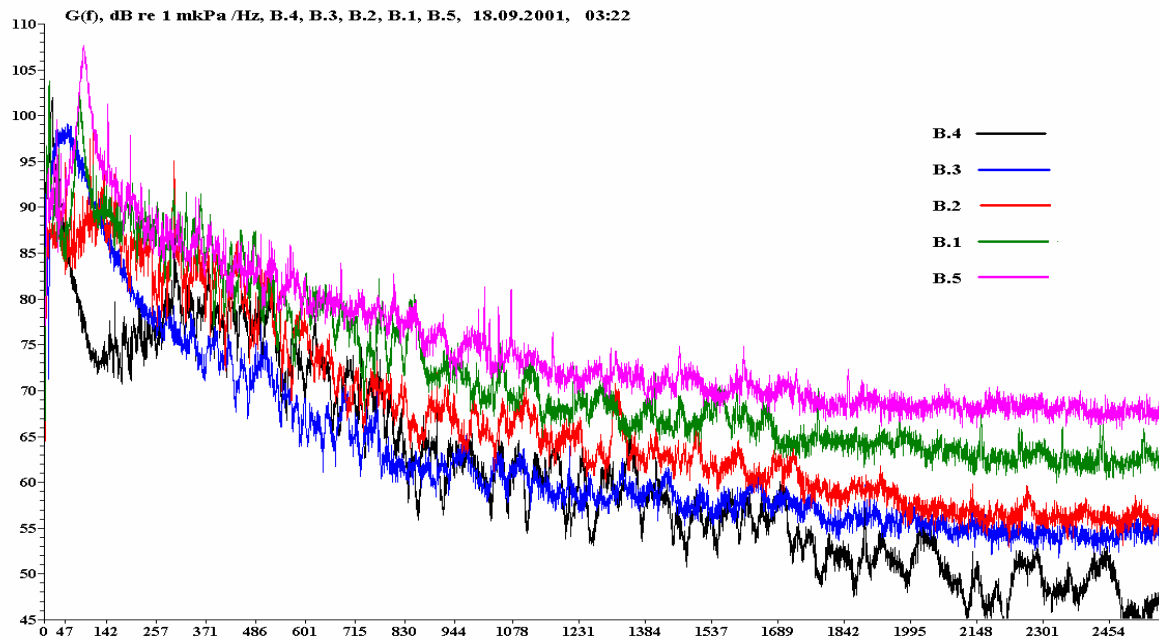
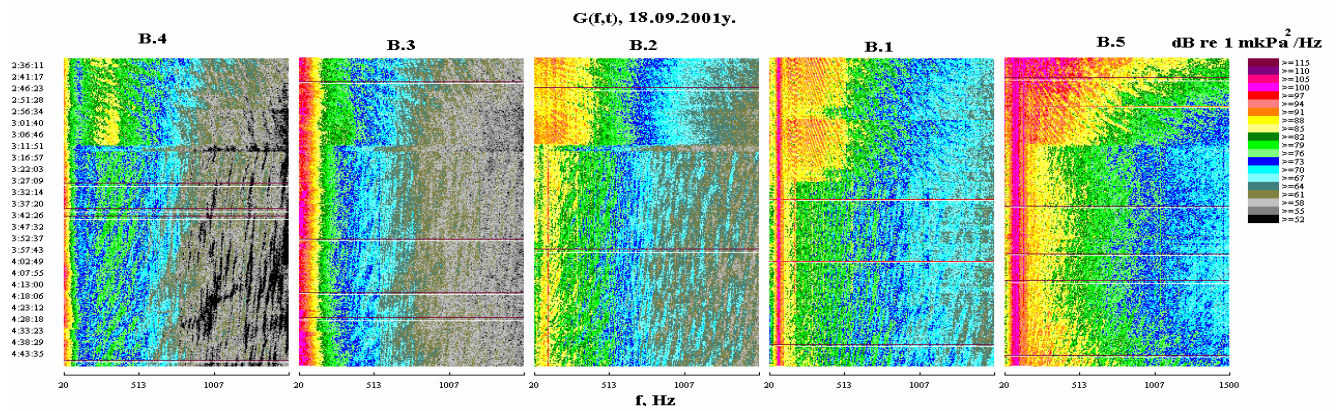


Figure 4.7 - Sonograms $G(f,t)$ and spectra $G(f)$ of acoustic background synchronously recorded at locations B.4, B.3, B.2, B1 and B.5 during the night of 18 September 2001.

The spectral levels of the noise at frequencies of 150-1300 Hz were approximately 20 dB higher at location B.5 than at location B.4. The spectra $G(f)$ at 04:30h (Figure 4.6) and at 04:04h (Figure 4.7) correspond to the acoustic background generated by the Molikpaq, the *Okha* and their support vessels anchored nearby. The spectra for locations B.5, B.1 and B.2 show a pronounced ~80 Hz peak, which was caused by internal cross feed within the AX-700 radio receiver²³.

4.2 Acoustic characterization of equipment on the Molikpaq platform

On the morning of 18 September two researchers were transferred from the *Irbis* to the Molikpaq via the support vessel *Smit Sakhalin*. Their primary objectives were to measure the acoustic signals emanating from equipment on the platform and collect information on the operating schedules and parameters for machinery that could be a potential source of noise. The measurements were conducted using the same 2-channel digital tape (DAT) recorder, two hydrophones and three amplifiers that were used to record acoustic signals on the *Griff* [Borisov et. al. 2002]. Since the coupling function between the equipment and the environment is not known, these measurements could not be used to determine the source level of sound emanating from the Molikpaq. Spectra of the acoustic noise recorded on the Molikpaq and displayed in the following figures were therefore not normalized and have no low frequency correction. This data is used only to analyze the spectral content of noise generated by equipment working on the Molikpaq.

The first acoustic measurements were made in the ballast chambers located near the hull of the Molikpaq, about 15 m below sea level. Molikpaq has four such chambers; two containing four pumps each, and two with two pumps each. All 12 pumps are the same (170 kW) model, nominally rotating at 1770 rpm a frequency of 29.5 Hz. During the measurements from 09:28h to 09:38h one hydrophone was lowered into water at the bottom of the ballast chamber, while the other lay in a puddle of water on the deck above the main beam.

²³ This electric induction is an inherent technical flaw of radio receivers of this type and cannot be corrected. In order to maintain the dynamic range necessary to measure acoustic signals in the presence of this noise, the preamplifier gain at low frequencies was decreased. This decrease was later compensated for by the use of a frequency corrector [Borisov et. al., 2002], however, this frequency corrector increases the gain at low frequencies for the induced noise as well as the acoustic signal.

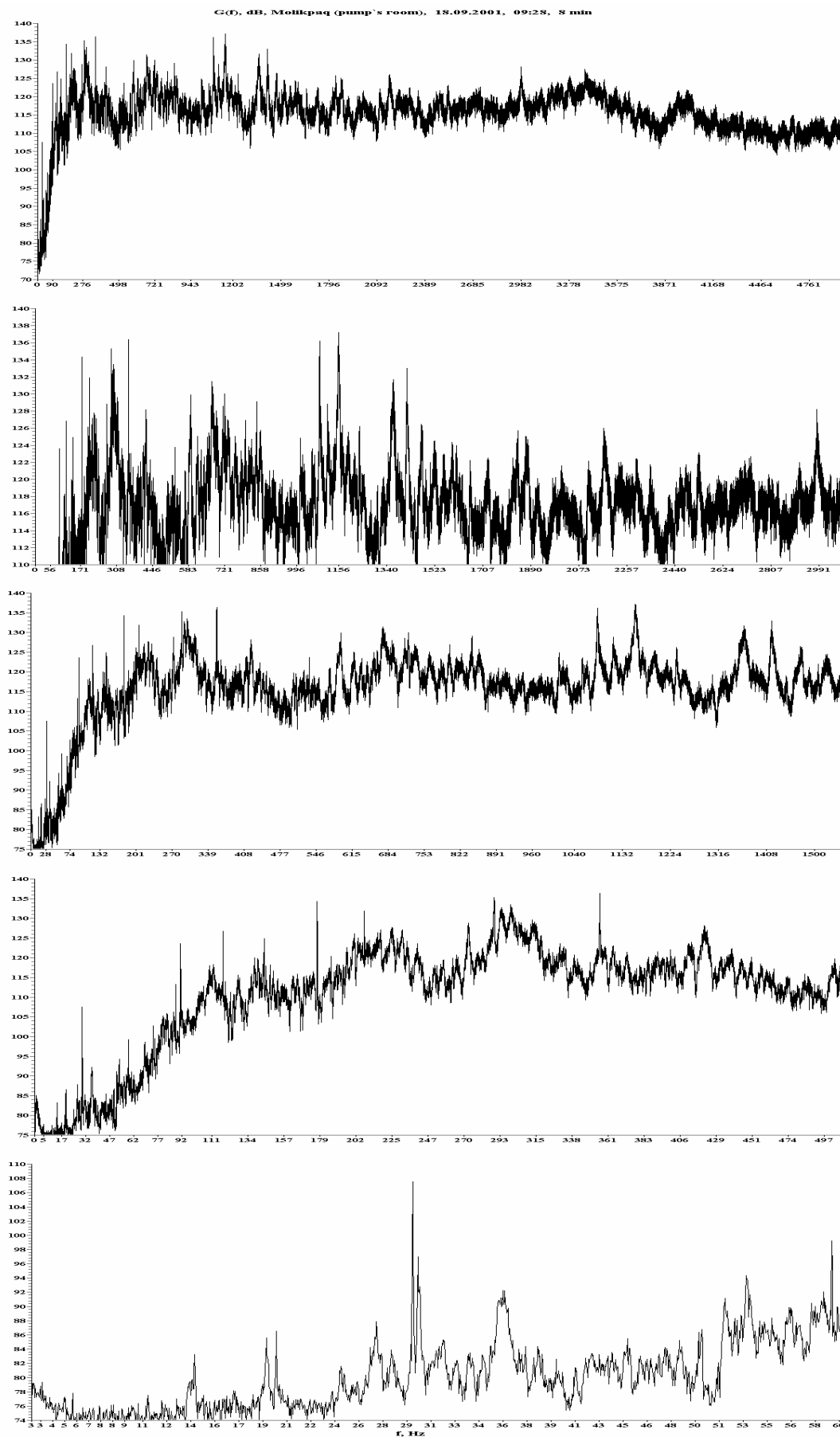


Figure 4.8 - relative spectra $G(f)$ of acoustic noises recorded in the ballast chamber of the Molikpaq at 09:30h on 18 September 2001.

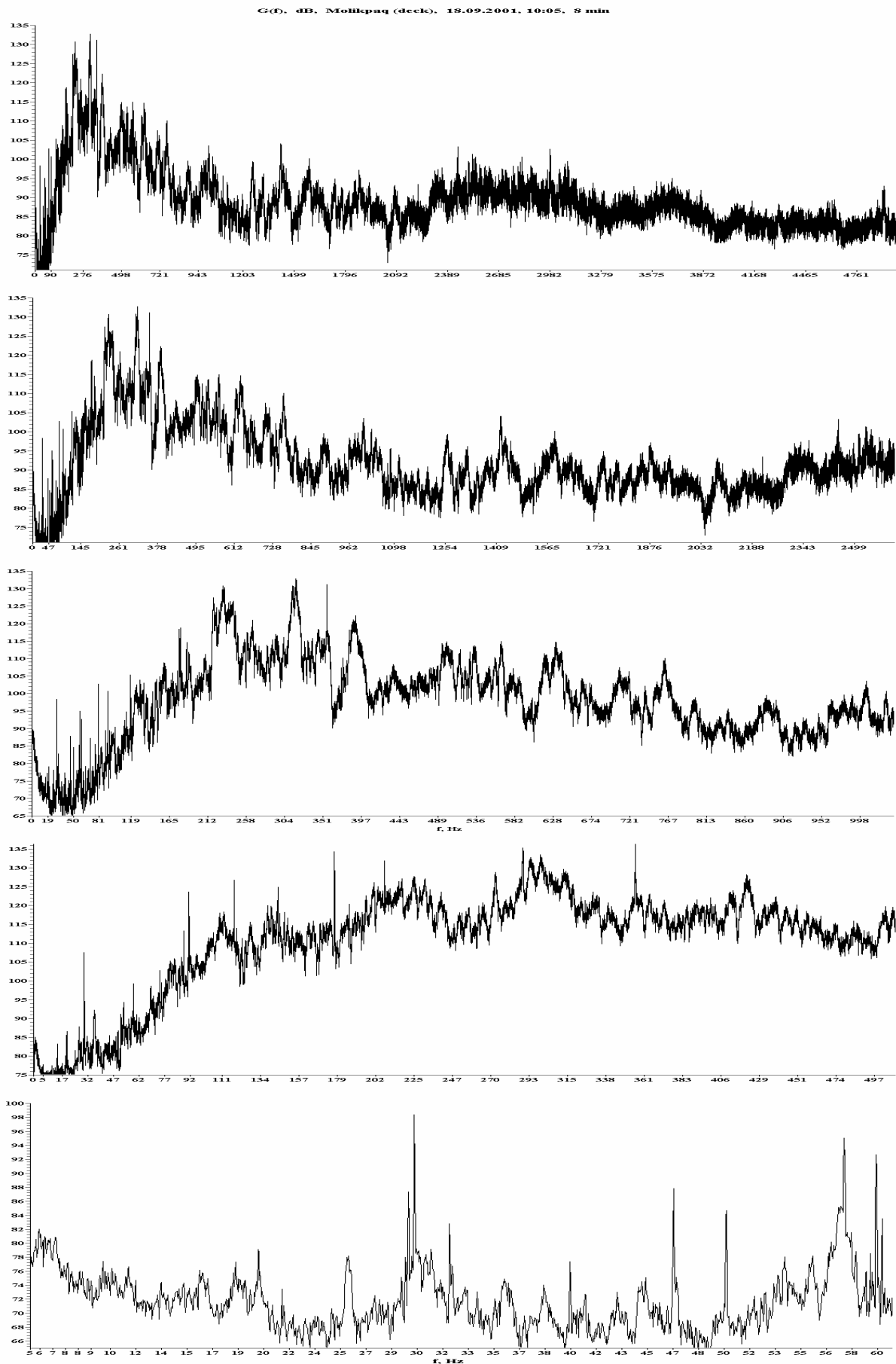


Figure 4.9 - Relative spectra $G(f)$ of acoustic noises recorded on the deck above the ballast chamber of the Molikpaq at 10:00h on 18 September 2001.

Figure 4.8 shows the spectra $G(f)^{24}$ of the data recorded by the hydrophone lowered into the water at the bottom of the ballast chamber. The spectrum has pronounced narrowband components, with tonal signals at frequencies of approximately 14, 20, 30, 59, 93, 128, 175, 205, and 360 Hz. Narrowband signals at higher frequencies (i.e. 1100, 1200, 1360, 1400 and 3000 Hz) are also present. Spectral levels of these tonal components are more than 25 dB higher than the level of the broadband noise, particularly at low frequencies²⁵.

Figure 4.9 shows the spectral analysis of data recorded by the hydrophone lying in a puddle of water on the main deck of the Molikpaq, above the ballast chambers at approximately sea level. The tonal component of the noise spectrum is clearly seen on Figure 4.9 as well as Figure 4.8.

Another potential source of acoustic noise on the Molikpaq is an injection pump. This pump includes a turbine and air compressor connected via a pressure regulator and is used to pump gas into the borehole. Sensors control the rotational speed (rpm), and amplitude of oscillation of the shafts. At 10:30h, two injection pumps operated with the following settings:

- Turbine 1 - 10560 rpm (176 Hz);
- Compressor 1 - 9630 rpm (160.5 Hz);
- Turbine 2 - 10290 rpm (171.5 Hz); and
- Compressor 2 - 9600 rpm (160 Hz).

The amplitudes of the oscillations of the shafts were:

- Turbine 1 - 33 μm ;
- Compressor 1 - 20 μm ;
- Pressure regulator 1 - 26 μm ;
- Turbine 2 - 31 μm ;
- Compressor 2 - 19 μm ; and
- Pressure regulator 2 - 20 μm .

²⁴ To allow the frequency resolution to be increased (<0.1 Hz) these spectra (Figures 4.8 and 4.9) have been computed over an analysis window of approximately 10 seconds. These ~10 second spectral estimates were averaged over 10 minutes.

²⁵ Note that since the spectra are not absolute spectra the numerical values of the spectral components are arbitrary and cannot be compared to calibrated absolute spectral values.

At 10:57h, the rotational speed did not change. The oscillation amplitudes of the shafts were:

- Turbine 1 - 32 μm ;
- compressor 1 - 20 μm ;
- pressure regulator 1 - 27 μm ;
- turbine 2 - 30 μm ;
- compressor 2 - 20 μm ; and
- pressure regulator 2 - 20 μm .

The spectra displayed in Figures 4.8 and 4.9 show that the equipment operating on the Molikpaq is a source of acoustic noise, this noise could be coupled to the water through the metal hull of the platform.

In the next chapter we will describe an experiment designed to determine if these noises do propagate from the Molikpaq platform, by trying to identify these noises among the acoustic noises registered synchronously at various distances from the Molikpaq.

5 Analysis of the Anthropogenic Acoustic Field from the Molikpaq Complex

This section describes the spectral, spatial and temporal variation in the acoustic field between the Molikpaq complex and the gray whale feeding area near Piltun Bay.

5.1 Characteristics of the acoustic field between Molikpaq and Piltun

Sonograms $G(f,t)$ of acoustic noise recorded synchronously at locations B.5, B.1, B.2, B.3, and B.4 will be shown during analysis of the spectral, spatial, and temporal characteristics of the acoustic field along the transect from Molikpaq to Piltun Bay. These sonograms give a temporal representation (12+ hours) of the variation in the acoustic environment along this transect. Quantitative estimates of the amplitude and frequency of characteristic acoustic signals at various locations and times will be presented based on calibrated spectra $G(f)$.

Figure 5.1 displays sonograms of acoustic noise synchronously measured at all five locations during 18 September 2001 (day). From these it can be seen that acoustic noise generated by both a moving vessel and another anchored near the Molikpaq propagate into the shallow part of the shelf and are clearly present in acoustic signals recorded at locations B.3 and B.4²⁶. Weather conditions during this experiment were as follows:

- 08:00h - No wind, ~1 m swell;
- 10:46h - No wind, ~1 m swell. Two vessels are present between the Molikpaq and *Okha*, two more vessels are located north of Molikpaq; and
- 15:20h - Some waves with white caps.

The spectra $G(f)$ displayed in Figure 5.2²⁷ correspond to the same time frame when the acoustic noise in the ballast chamber of the Molikpaq platform was recorded (Figure 4.8). Unfortunately, at the same time a vessel was working near the Molikpaq platform. It is probable therefore, that the striped spectra (for locations B.5, B.1, and B.2), at frequencies below 100 Hz and the narrowband noise at frequencies between 100-140 Hz (also seen at location B.4) were generated by the vessel.

²⁶ It should be noted that the high amplitude low frequency noise recorded at location B.3 and to a lesser extent B.4 are caused by flow noise (pseudo noise), these amplitudes not a true representation of the acoustic field in the area.

²⁷ The spectra in Figure 5.2 are high-resolution spectra. To increase the frequency resolution (<0.1 Hz) these spectra have been computed over an analysis window of approximately 15 seconds. These spectral realizations are therefore not absolute spectra [dB re 1 $\mu\text{Pa}^2/\text{Hz}$] but relative spectra. These ~15 second spectral estimates were then averaged over 16 minutes.

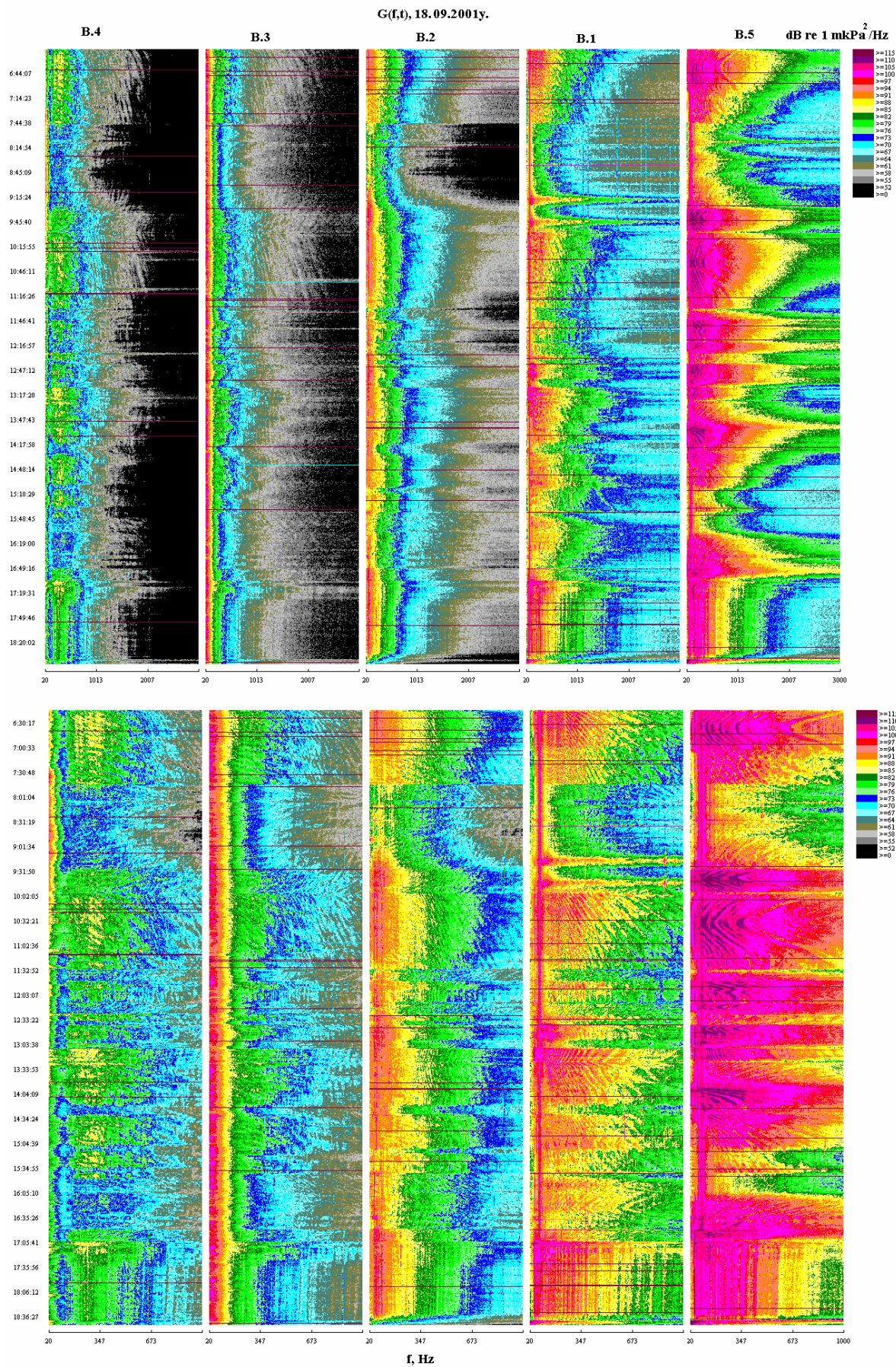


Figure 5.1 - Sonograms $G(f,t)$ of acoustic noise synchronously recorded at locations B.4, B.3, B.2, B.1 and B.5 during 18 September 2001 (day).

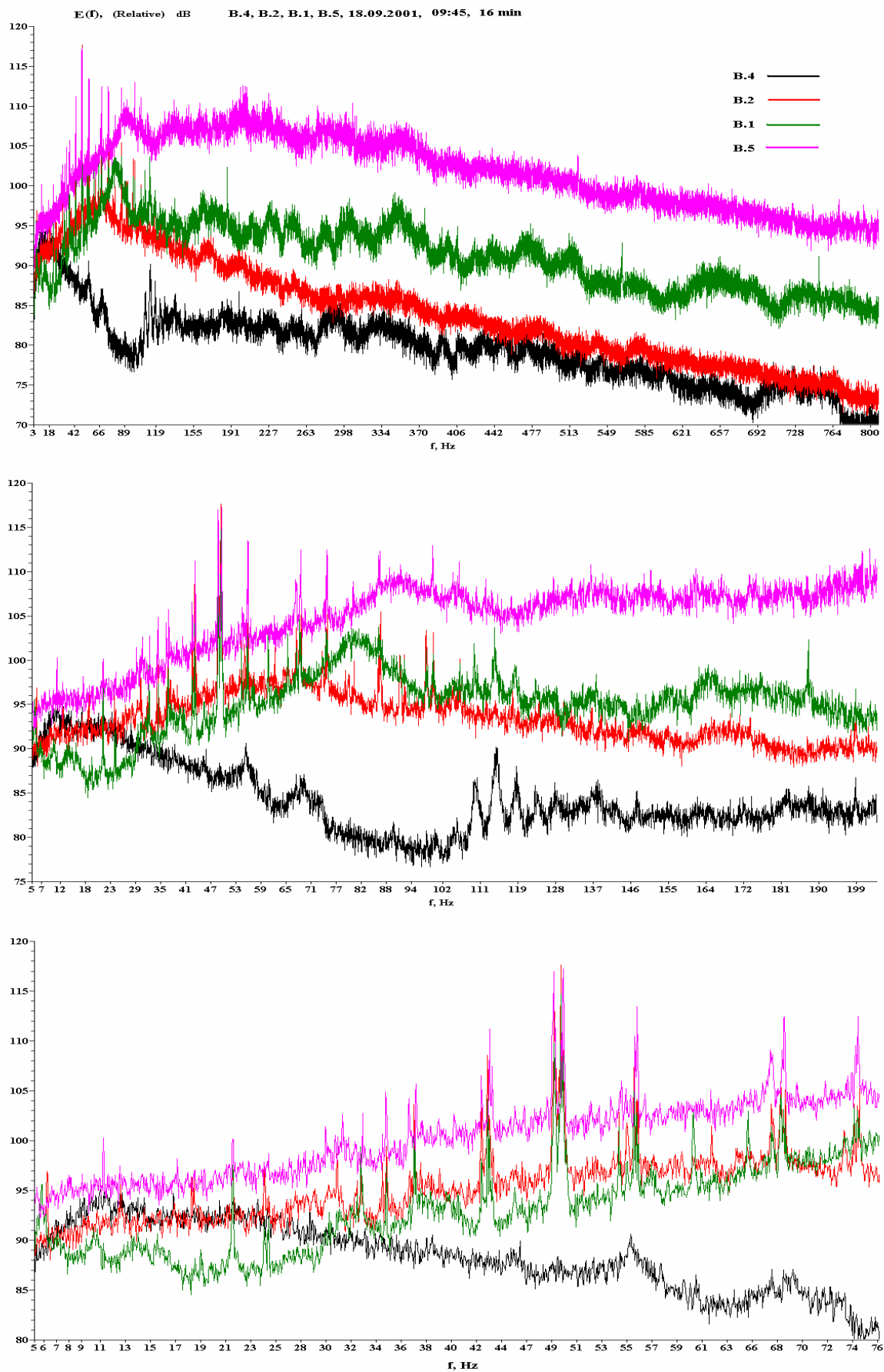


Figure 5.2 - Relative spectra $E(f)$ of acoustic noise synchronously recorded at locations B.4, B.3, B.2, B.1 and B.5 while the signal was recorded at Molikpaq.

In the low frequency part of the spectrum shown in Figure 5.2 there are tonal signals at frequencies of 12, 22, and 24 Hz, but the approximately 30 Hz signal recorded on the Molikpaq (Figure 4.8), was not seen. The source of the strongest peak at 50 Hz is unknown. However, since the peak is bimodal, it is possible that multiple generators on support vessels may have caused the peak. The precise location of these vessels is not known.

The spectra displayed in Figure 5.3 quantitatively characterize the variability in the acoustic background along the transect (B.5 to B.4). The spectra $G(f)$ for 08:28h and 08:43h correspond to times when there was no visible activity around the Molikpaq platform and the noise level was lower. The high amplitudes seen at low frequencies on B.4 between 07:30h and 10:30h (Figure 5.1) are not correlated with any other buoy and are probably wind or flow noise. The spectrum $G(f)$ at 10:37h corresponds to the time when the *Smit Sakhalin* could be seen moving from the Molikpaq platform towards the *Okha*. Complex acoustic signals with low amplitude striped spectra at frequencies between 500-1300 Hz were periodically observed at all locations along the transect (Figure 5.4), these signals sometimes lasted over 10 minutes. The spectral levels of these tonal components could exceed the broadband noise levels by over 10 dB. Interestingly, certain tonal components clearly seen in the spectra for locations B.5, B.1, and B.2 are not visible in the spectrum of the signal registered synchronously at location B.4, and vice versa. This would indicate that noise from the Molikpaq area is attenuated prior to reaching the Piltun gray whale area, and that some of the noise recorded in the Piltun area emanates from a source distinct from the Molikpaq (perhaps the Piltun lighthouse).

Figure 5.5 shows sonograms $G(f,t)$ of acoustic noise synchronously recorded at locations B.4, B.3, B.2, B.1, and B.5 during the night of 19 September 2001. These sonograms indicate that the noise sources were stationary, and that the acoustic background was dominated by noise from anchored vessels near the Molikpaq platform including the *Irbis*.

On 21 September a strong northerly wind (15-20 m/s) and high sea state (Beaufort 5-6) caused the *Irbis* to raise anchor at 13:00h and sail northwards towards location 52°54.27' N, 143°31.06' E. At 15:37h the *Irbis* reached its new location and turned onto a bearing of 183°. By 16:09h the *Irbis* was sailing at 7.4 knots (with its main shaft revolving at 450 rpm).

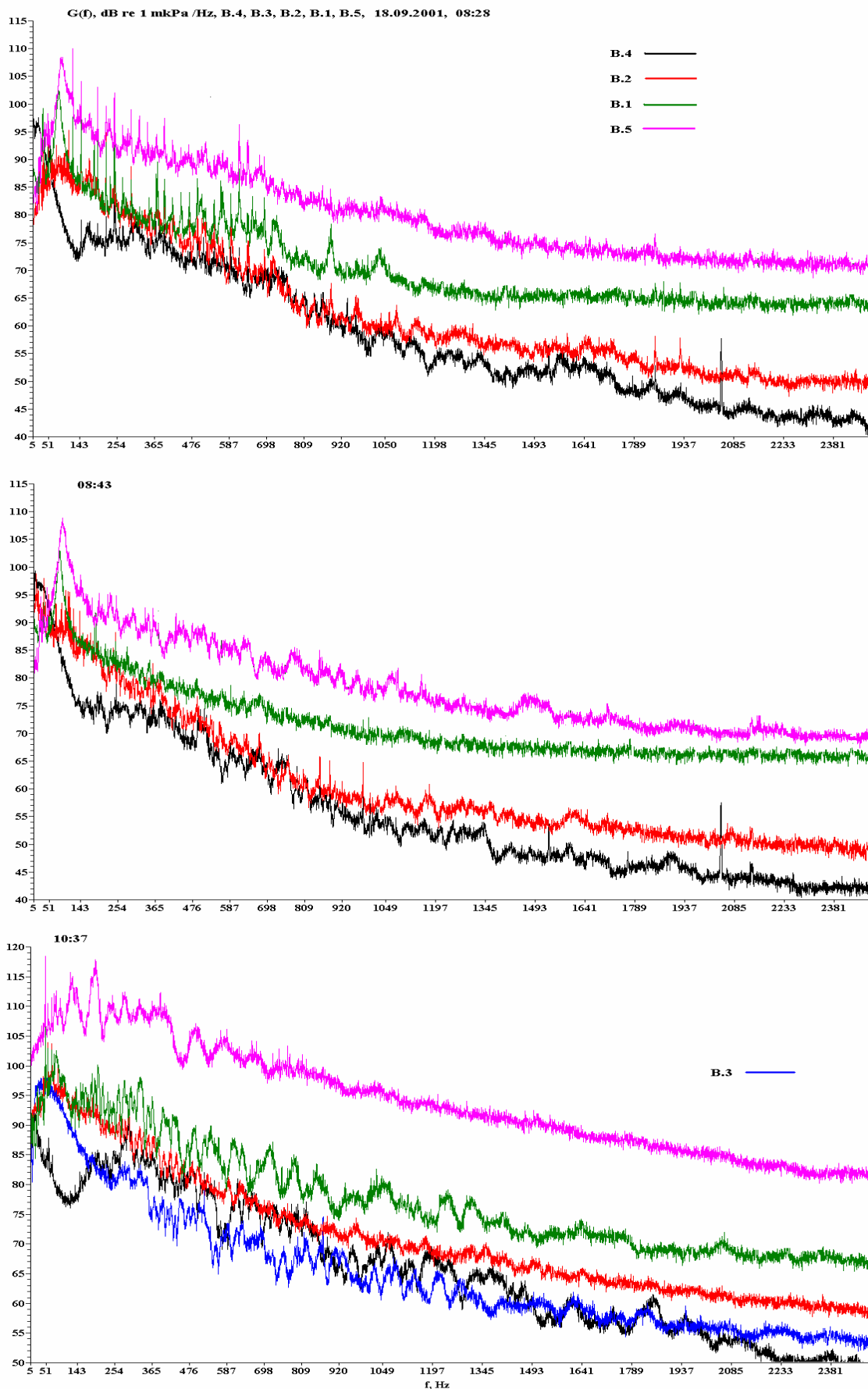


Figure 5.3 - Spectra $G(f)$ of acoustic noise synchronously recorded at locations B.4, B.3, B.2, B.1 and B.5 during 18 September 2001.

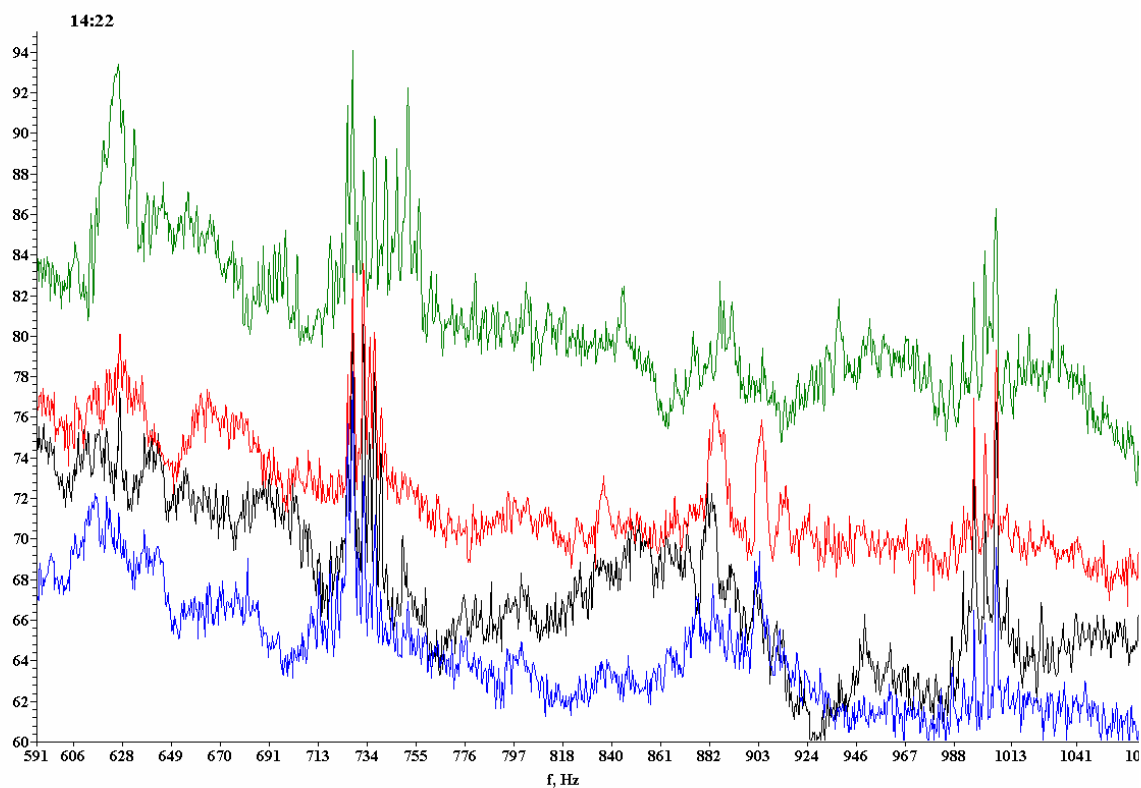
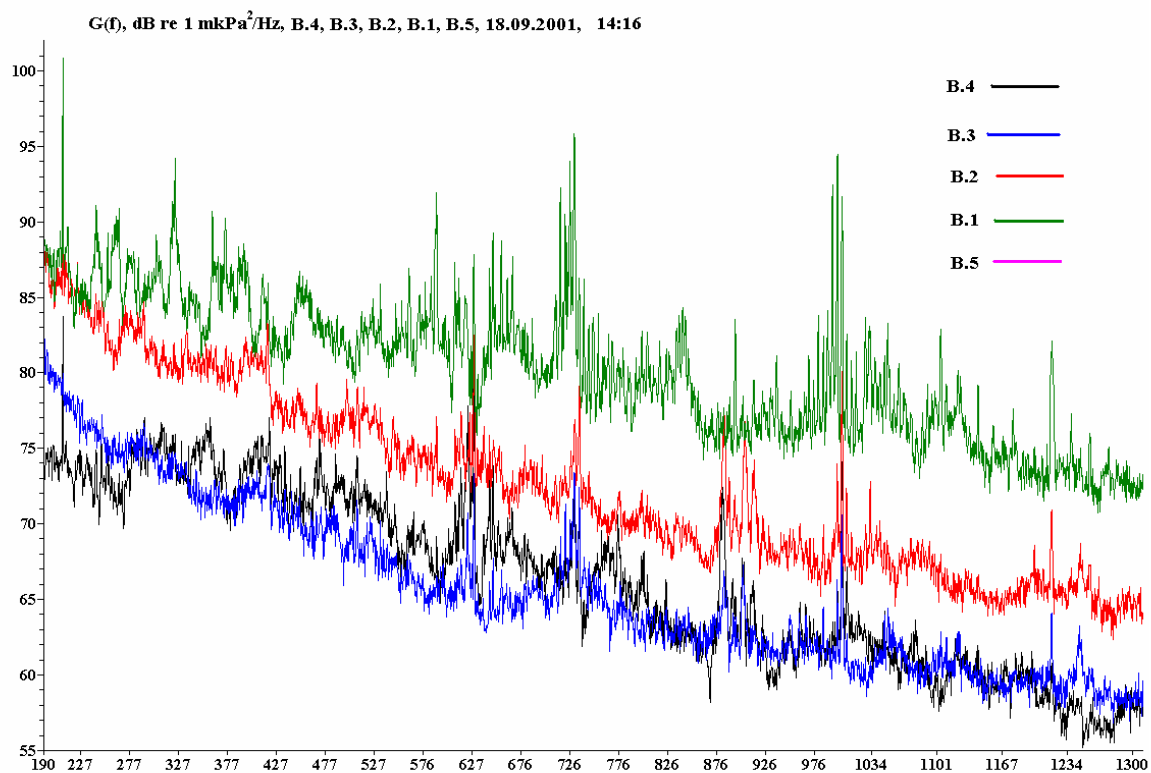


Figure 5.4 - Spectra $G(f)$ of tonal acoustic noise synchronously recorded at locations B.4, B.3, B.2, B.1 and B.5 during 18 September 2001.

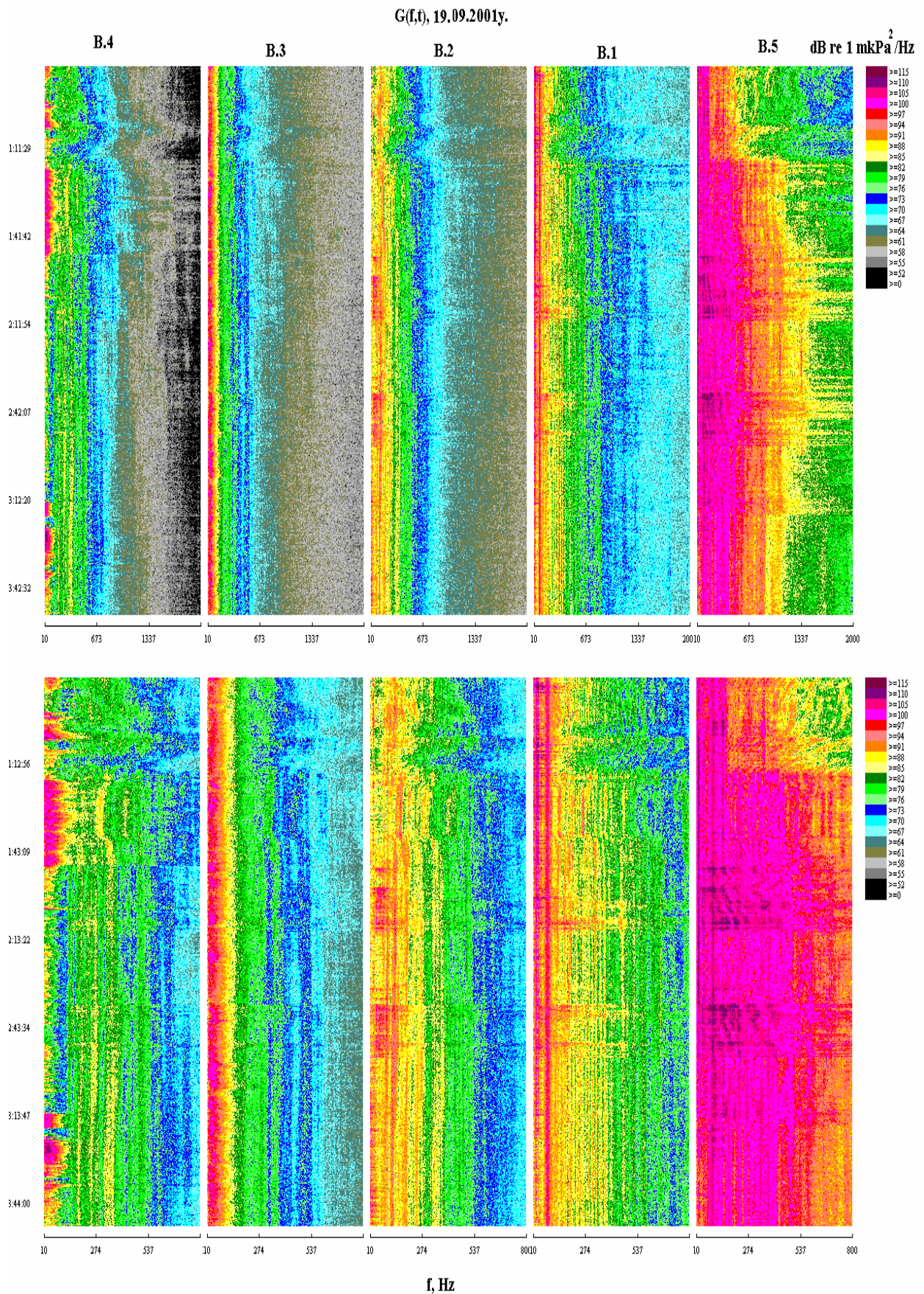


Figure 5.5 - Sonograms $G(f,t)$ of acoustic noise synchronously recorded at locations B.4, B.3, B.2, B.1 and B.5 during the night of 19 September 2001.

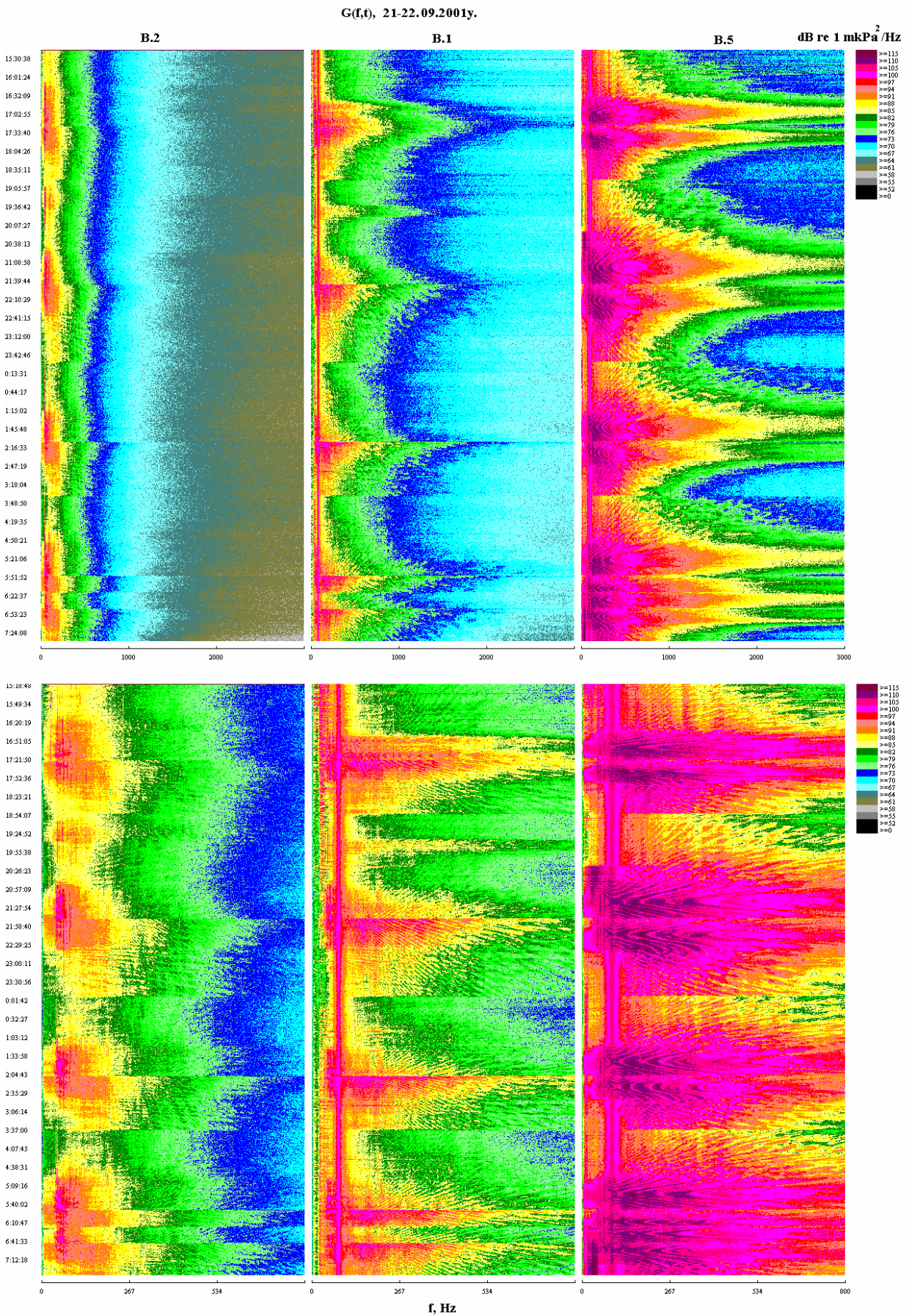


Figure 5.6 - Sonograms $G(f,t)$ of acoustic noise synchronously recorded at locations B.2, B.1 and B.5 during 21-22 September 2001.

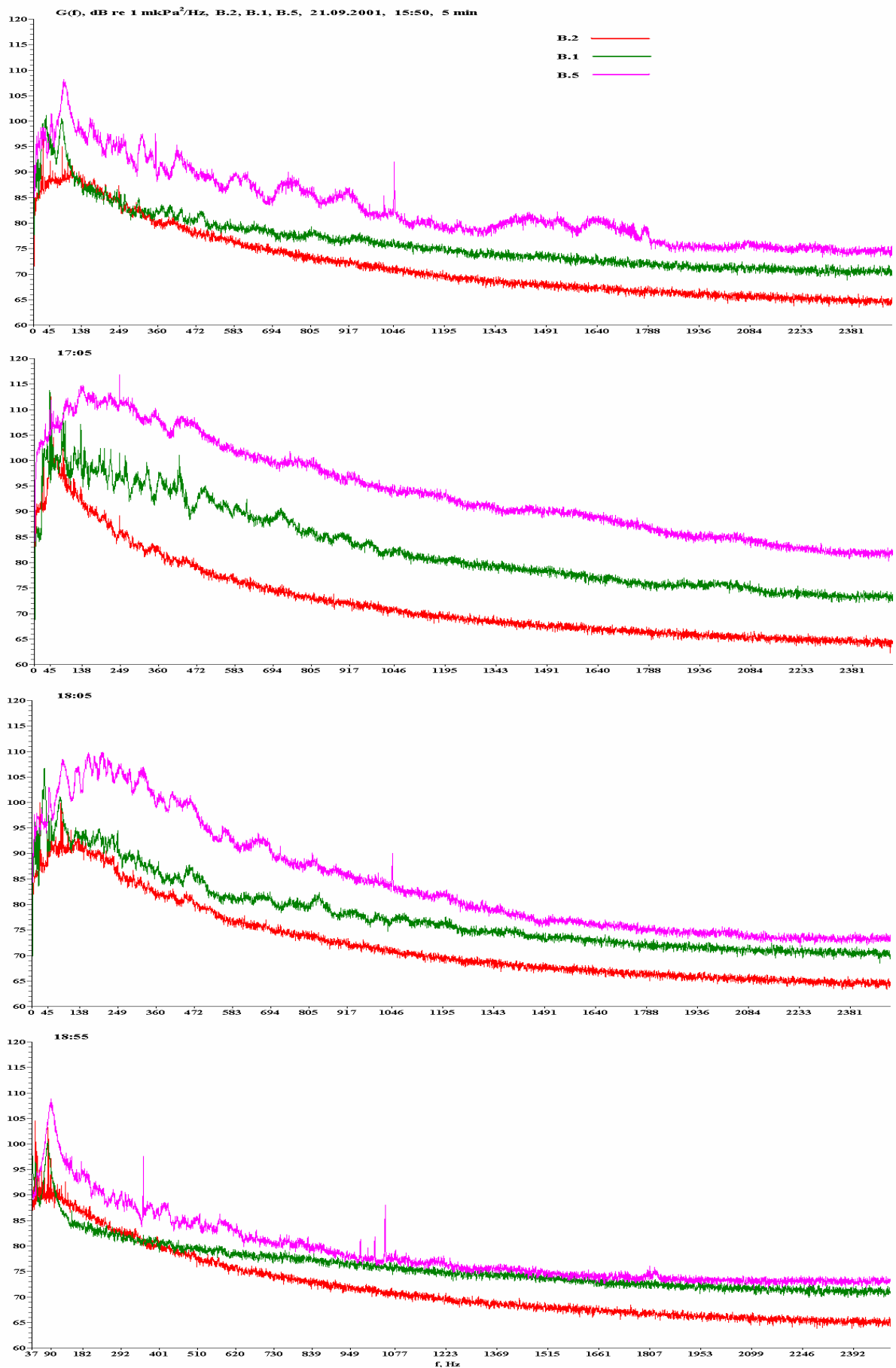


Figure 5.7 - Spectra $G(f)$ of acoustic noise synchronously recorded at locations B.2, B.1 and B.5 at 15:50h, 17:05h, 18:05h and 18:55h on 21 September 2001.

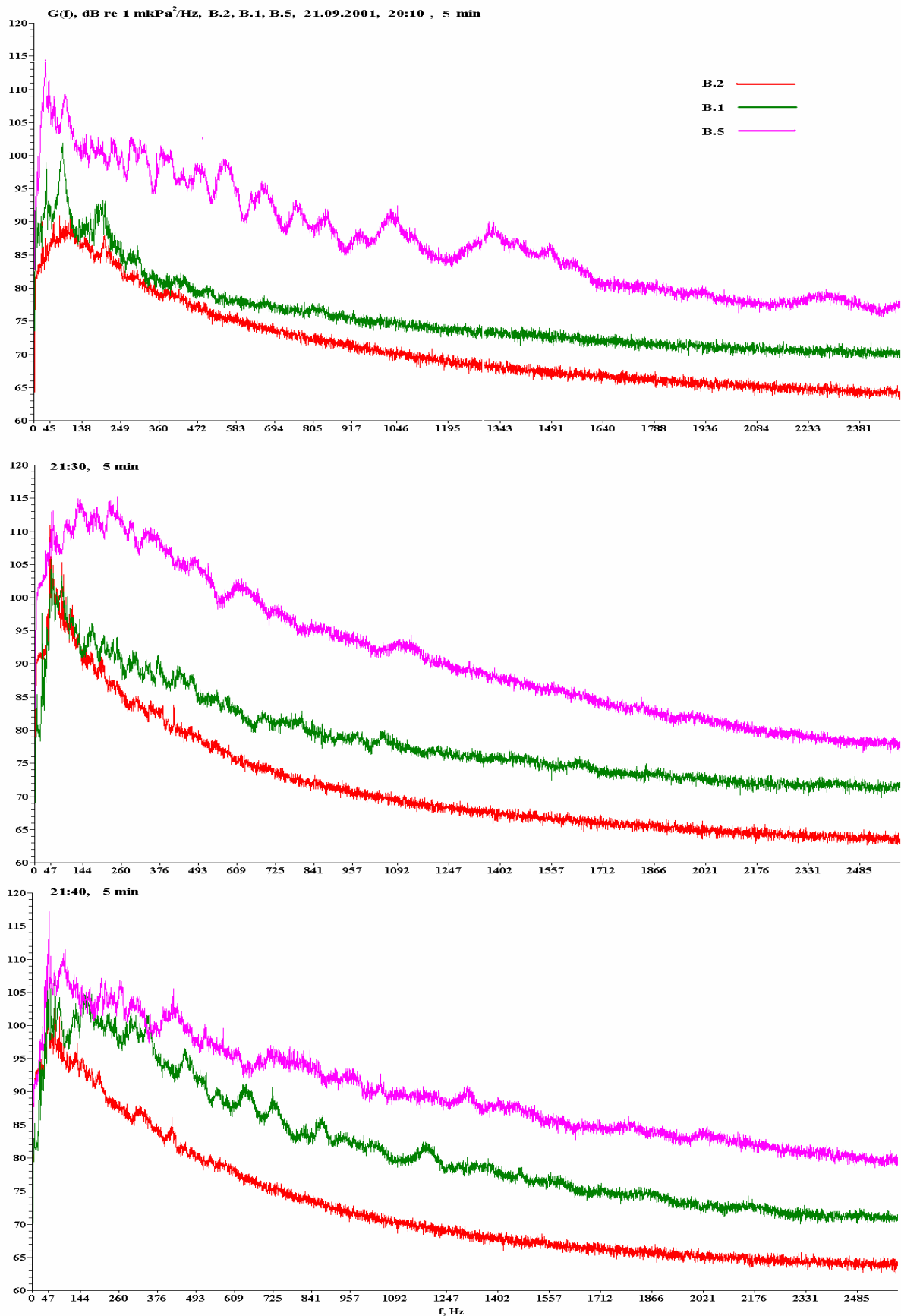


Figure 5.8 - Spectra $G(f)$ of acoustic noise synchronously recorded at locations B.2, B.1 and B.5 at 20:10h, 21:30h and 21:40h on 21 September 2001.

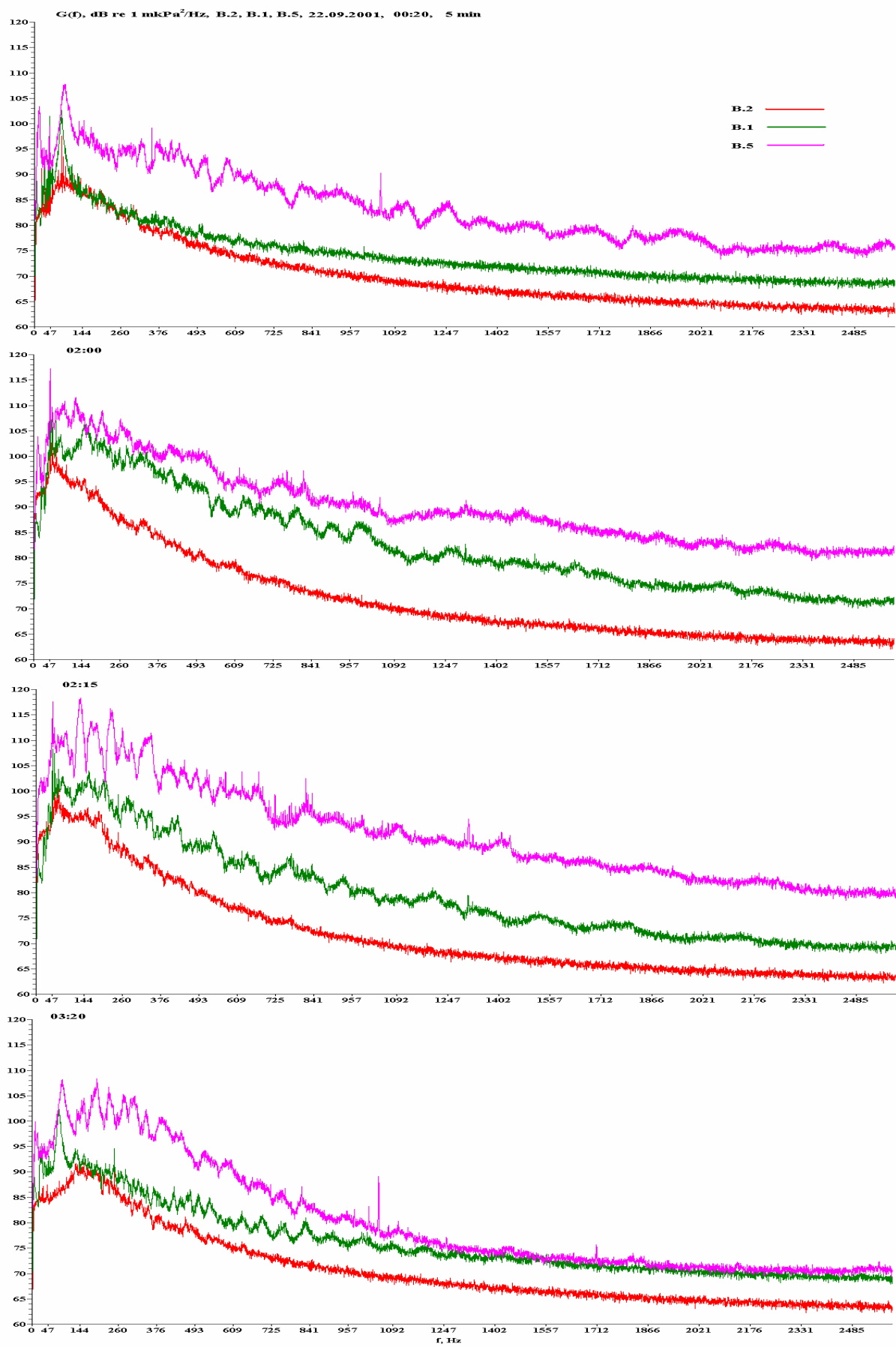


Figure 5.9 - Spectra $G(f)$ of acoustic noise synchronously recorded at locations B.2, B.1 and B.5 at 00:20h, 02:00h, 02:15h and 03:20h on 22 September 2001.

From 21:55h on 21 September to 07:15h on 22 September the *Irbis* was sailing between locations $\tau.1$ and $\tau.2$ as shown on Figure 1.1, all other vessels were anchored. Figure 5.6 shows sonograms of the noise field synchronously recorded at locations B.5, B.1, and B.2 as the *Irbis* was maneuvering in the storm (Figure 1.1). The sudden changes in the frequency interference patterns seen in Figure 5.6 are caused by the *Irbis* traversing the hydrophones and making sharp turns.

The noise field generated by a moving vessel is generally more intensive behind the vessel. The spectra $G(f)$ displayed in Figures 5.7 to 5.9 are quantitative estimates of the levels of noise under high winds and sea states and at various distances from the *Irbis*.

Weather conditions and vessel traffic during September 22 (day) were as follows:

- 07:15h - *Irbis* casts anchor;
- 07:52h - Sunny, some whitecaps, there are three vessels near the Molikpaq;
- 09:28h - *Miss Sybil* sails from the *Okha* to the *Irbis*;
- 09:57h - *Miss Sybil* shuts down its engine; tanker *Primorye* approaches from the east;
- Both 'Smits' are anchored stern to stern near the *Irbis*; *Primorye* stopped;
- 12:25h - *Primorye* is ordered to raise anchor and sail to the mooring site;
- 13:09h - *Miss Sybil* sails towards *Primorye*; *Smit Sakhalin* sails towards the *Okha*; the *Smit Seeboo* (sp) is anchored;
- 13:48h - *Primorye* has commenced mooring;
- 14:55h - Work boat *Malysh* from the *Okha* leads a tugboat; *Smit Seeboo* moves towards Molikpaq; *Smit Sakhalin* is at the rear of *Primorye* holding it;
- 15:16h - The *Okha* and *Primorye* approach within 100 m; the chain of the Molikpaq, *Okha*, *Primorye*, and *Smit Sakhalin* stretches from north to south;
- 16:45h - Off-loading of oil begins;
- 17:05h - *Irbis* starts its main engine;
- 17:20h - *Irbis* starts moving towards Molikpaq;
- 17:38h - *Irbis* stops 300 m north of the Molikpaq;
- 18:33h - *Irbis* sails at a bearing of 262°; a second tanker appears on the horizon;
- 18:50h - *Irbis* casts its anchor; and
- 21:30h - The current switches 180° and the chain of the vessels does the same.

Figures 5.10 and 5.11 show the spectral analysis of acoustic noise synchronously recorded at locations B.2, B.1, and B.5 during the time frame described above. Unfortunately the sonobuoys at locations B.4 and B.3 sustained damage to their antennae during the storm and stopped working; only data for locations B.2, B.1, and B.5 are therefore available.

The maximum level of acoustic noise recorded at locations B.2 and B.1 were during the mooring of the *Primorye* to the *Okha* (Figure 5.10). This noise level depends on the orientation of the chain of the *Okha*, *Primorye*, and *Smit Sakhalin*, which is controlled by the direction of the tidal current. The main noise source was the tugboat *Smit Sakhalin*, whose engines were continuously running to hold the chain of tankers in position against the current. When the current was running from south to north, the *Smit Sakhalin* was located closer to the sonobuoy, and the level of recorded noise was higher.

While the oil was being off-loaded (Figure 5.11), tonal components and broadband noise were recorded at locations B.1 and B.5. Tonal components at frequencies below 300 Hz could exceed 115 dB (at location B.5). The complex frequency interference structure of the acoustic field at location B.2 (14m water depth, 15.5 km from Molikpaq) is significantly less pronounced at frequencies above 500 Hz. However, the low frequency tonal components (40-130 Hz) recorded at location B.2 can sometimes exceed the levels of those components recorded at location B.1 (20 m water depth, 8.3 km from Molikpaq)²⁸. Figure 5.11 (21:34h and 21:46h) shows complex acoustic signals with striped spectra, the signals were synchronously recorded at three locations B.5, B.1 and B.2).

The off-loading of oil from the *Okha* to the tanker *Primorye* was completed by 03:00h on 23 September 2002, by 08:20h the *Primorye* had left the *Okha*, a second tanker then began mooring to the *Okha*. Figure 5.12 displays a sonogram of acoustic measurements recorded synchronously at locations B.2, B.1, and B.5 during the mooring of the second tanker and the off-loading of oil from the *Okha* to the tanker.

²⁸ It is uncertain whether this is a real transmission effect or an artifact of the calibration accuracy of the analog sonobuoys at frequencies below 100 Hz.

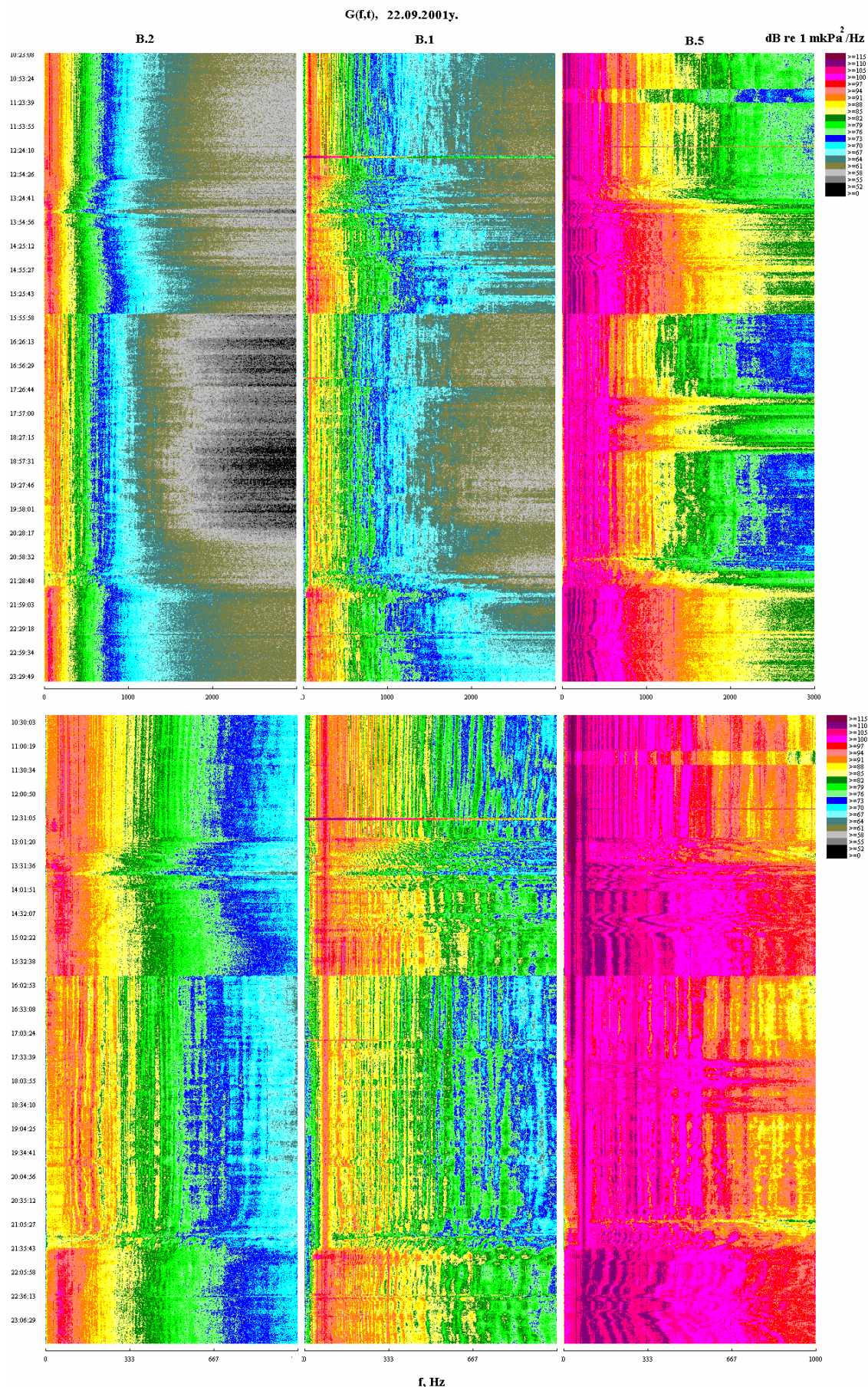


Figure 5.10 - Sonograms $G(f,t)$ of acoustic noise synchronously recorded at locations B.2, B.1 and B.5 during 22 September 2001 (day).

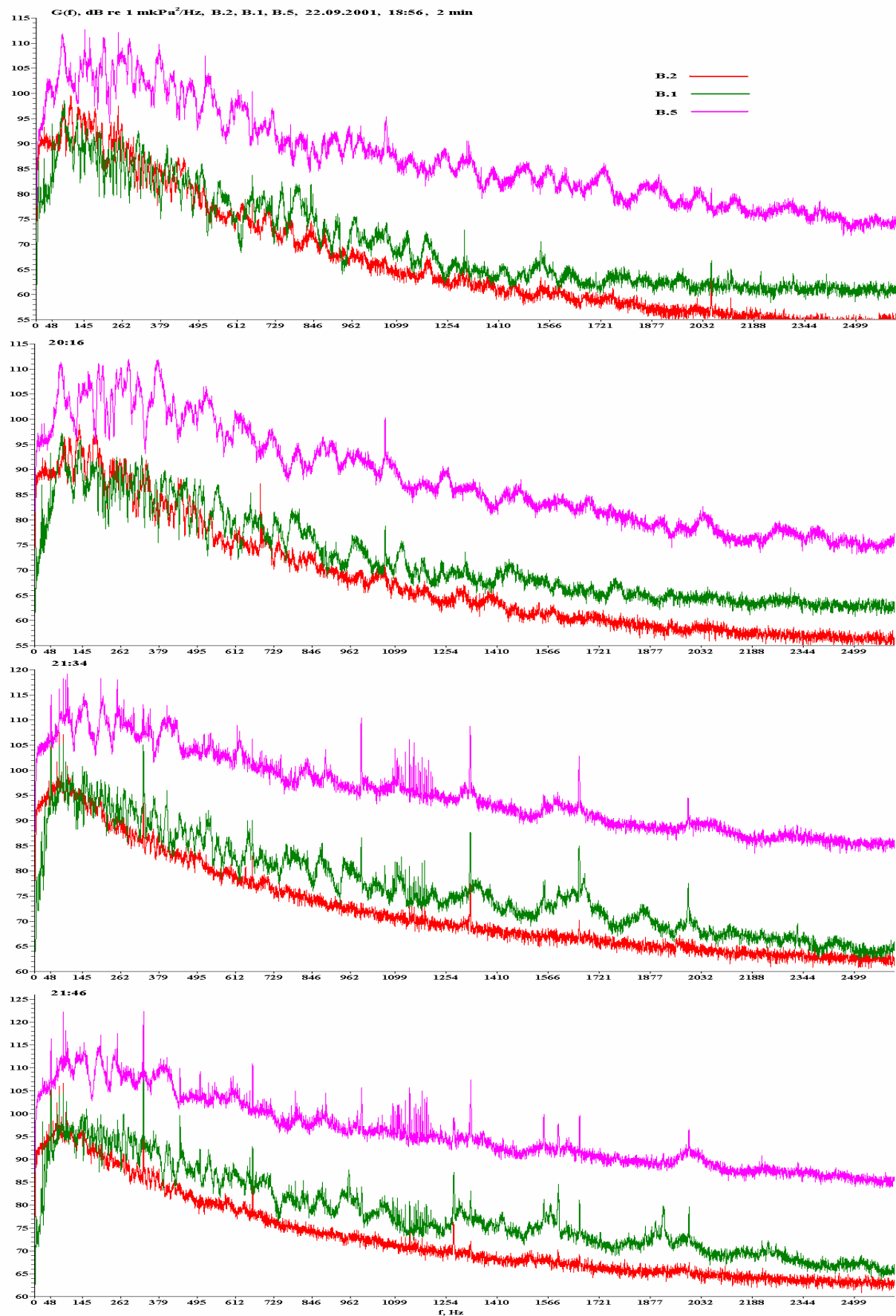


Figure 5.11 - Spectra $G(f)$ of acoustic noise synchronously recorded at locations B.2, B.1 and B.5 at 18:56h, 20:16h, 21:34h and 21:46h on 22 September 2001.

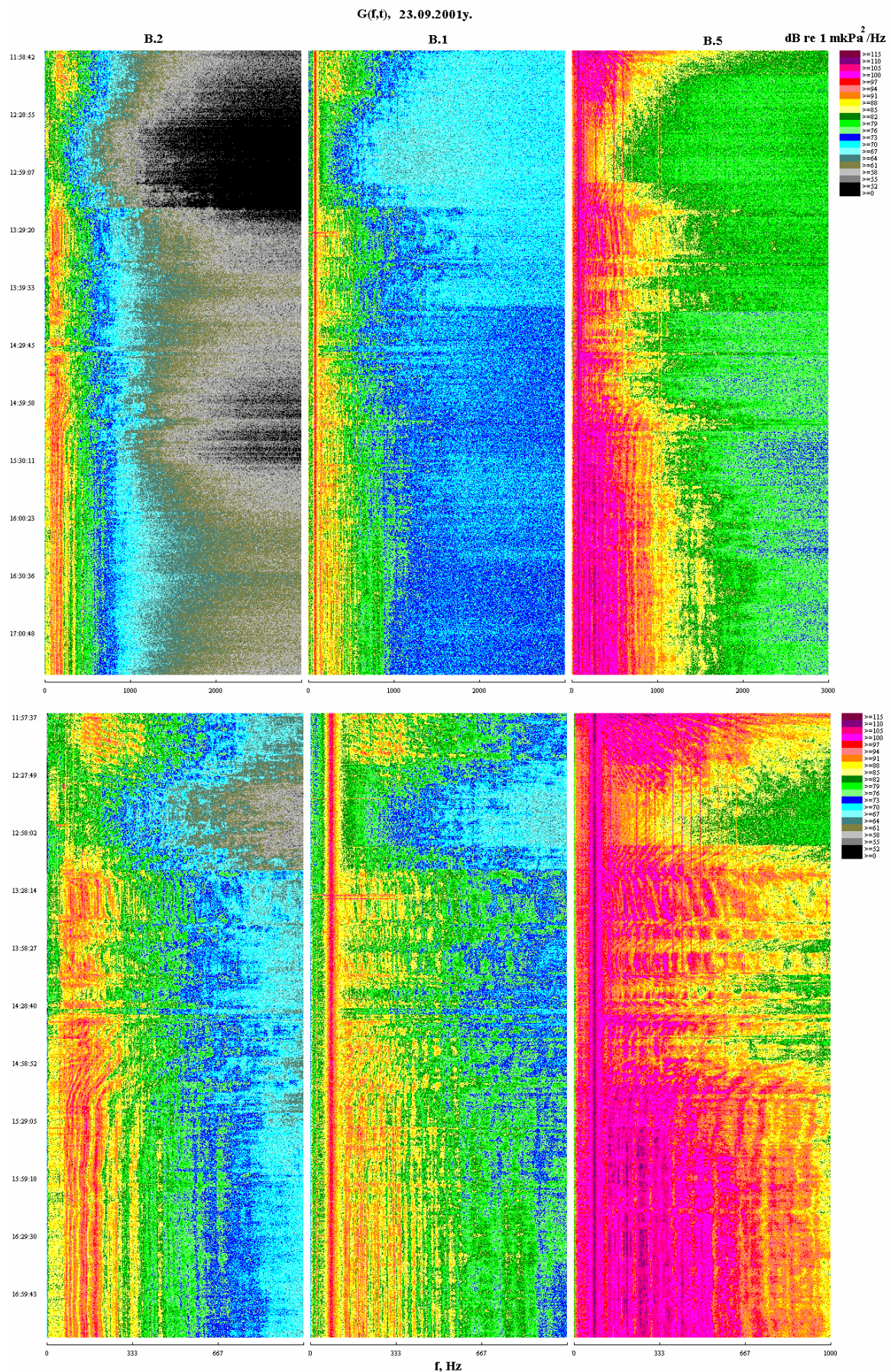


Figure 5.12 - Sonograms $G(f,t)$ of acoustic noise synchronously recorded at locations B.2, B.1 and B.5 during 23 September 2001 (day).

6 Conclusions

1. The Molikpaq platform and Vityaz oil complex has pronounced tonal and narrowband acoustic components with spectral levels 10-15 dB higher than the level of the broadband noise.
2. Tonal spectral components at frequencies below 30 Hz have been recorded near the field.
3. Measurements of the acoustic background in the area of Piltun Bay indicate that the most intensive acoustic noise source for frequencies below 1000 Hz were support vessels; the intensity of the broadband noise increased by 15-20 dB when one of these support vessels was moving. The off-loading of oil generates more noise due to the number of vessels involved.
4. Anthropogenic acoustic noise generated by stationery and moving industrial sources are consistently recorded in the gray whale feeding area off the mouth of Piltun Bay. However, this noise has been significantly attenuated prior to reaching this area. The spectral levels of tonal and narrowband signals for frequencies below 500 Hz recorded at both locations B.3 (11 m) and B.4 (10 m) do not exceed 85 dB re 1 $\mu\text{Pa}^2/\text{Hz}$.

7 Future plans

The acoustic studies conducted in the area of the Molikpaq in 2002 confirmed the value of acoustic monitoring using autonomous sonobuoys. The signals from these sonobuoys can be synchronously recorded to allow more effective analysis of the data. However, concerns over the low frequency response and dynamic range of the analog sonobuoys demonstrated the need to develop new digital equipment, with a greater dynamic range.

POI has significant experience in the design, development, manufacturing and operation of digital sonobuoys, transmitting the acoustic signals in a digital format [Bondar et. al. 1993]. The key limitation to the transmission of digital acoustic data by a radio-channel, is the bandwidth of radio receivers. A digital sonobuoy with a 16-bit ADT (96 dB) and encoding, can only transmit signals between 0-2500 Hz. If the 12-bit ADT (72 dB) is used, then the frequency range is 0-4000 Hz. One of the main advantages of digital encoding is the elimination of system noise and electric induction, which are particularly significant at low frequencies and preclude accurate measurements of infrasounds by analog sonobuoys. This widening of the dynamic range will decrease the transmission range for the sonobuoys, even after a doubling of the transmission power. The combination of digital and analog sonobuoys will allow accurate acoustic measurements from 1 to 10,000 Hz (digital 1-2500 Hz, analog 200-10,000 Hz). Digital sonobuoys using piezo-electric accelerometers will allow acoustic measurements in the range from 0.07-80 Hz²⁹.

For accurate field studies of transmission loss a low-frequency resonance electromagnetic transducer is being developed.

Due to the operating failure of the buoys at locations B.3 and B.4 and the poor low frequency response of the analog sonobuoys, an effective analysis of broadband transmission loss could not be undertaken. In the 2002 field season a more robust estimation of broadband transmission loss between the Molikpaq platform and the mouth of Piltun Bay will be undertaken.

²⁹ It should be noted that the high amplitude low frequency noise recorded on sonobuoys deployed in shallow water (e.g. location B.3) is caused by flow noise (pseudo noise). These noises are generated by the interaction of the hydrophone and the current flow and are not present in the absence of the sensor, they are difficult to mitigate against and will probably be present even on data recorded by more advanced systems.

8 Acknowledgements

The authors would like to thank the V.I. Il'icev Pacific Oceanological Institute (POI), Far East Branch Academy of Sciences of Russia (FEB RAS), (Тихоокеанский океанологический институт им. В.И. Ильичева ДВО РАН), for permission to conduct this work.

The authors would also like to acknowledge the following personnel from POI, who while they did not contribute to the report, contributed significantly to the success of the program in the field. Sc. R.A. Korotchenko (Коротченко Р.А.); engineers: E.A. Maslennikov (Масленников Е.А.), V.V. Lihachev (Лихачев В.В.), D.G. Kovzel` (Ковзель Д. Г.).

The authors also wish to thank the crew of the *Irbis* for their hospitality and assistance while conducting acoustic measurements in the vicinity of Molikpaq.

Finally the authors would like to thank Dr. Sc. G.I. Dolgih (Долгих Г. И.)(POI), Dr. Richard T. Houck, Dr. Warren S. Ross (ExxonMobil Upstream Research Co.), and Dr. H. Rodger Melton (ExxonMobil Upstream Research Co.) for reviewing this report.

Our special thanks go to the investment companies, their employees and consultants, without whom the present work could not have been conducted. These include:

LGL Ltd. - Dr. S.B. Yazvenko and Dr. S.R. Johnson

Exxon Neftegas Ltd. - M.R. Jenkerson, C.R. Martin and H.R. Melton

Sakhalin Energy Investment Company Ltd. - J.C. Robinson and S. Balytsok

9 Authors

From the V.I. Il'icev Pacific Oceanological Institute, Far East Branch, Academy of Sciences of Russia:

Sc. S.V. Borisov (Борисов С.В.)

Sc. A.V. Gritsenko (Гриценко А.В.)

Dr. Sc. A.N. Rutenko (Рутенко А.Н.)

Sc. A.V. Hodzevich (Ходзевич А.В.)

10 Bibliography

- Bondar` L.F., Gritsenko A.V., Zakharov V.A., Kovzel` D.G. and Rutenko A.N. Digital radio-telemetry system for the collection and results of its application in studies of sea reverberation characteristics // *Acoust. Phys.*, 1993, vol.39, no.2, pp.118-122
- Borisov S.V., Gritsenko A.V., Jenkerson M.R., Rutenko A.N., and Hodzevich A.V. (2002) Evaluating and Monitoring Acoustic Transmission from the Odoptu 3D seismic Survey 5 August - 9 September, 2001; Sakhalin, Russian Federation // Pacific Oceanological Institute (FEB RAS) report for Exxon Neftegas Ltd.
- Cummings W.C., Thompson P.O., and Cook R (1968) Underwater sounds of migrating gray whales, *Eschrichtius glaucus* (Cope) // *J. Acoust. Soc. Am.* Vol. 44. no. 5. P. 1278-1281.
- Hilton-Taylor, C. 2000. IUCN Red List of Threatened Species. IUCN/SSC, Gland, Switzerland and Cambridge, UK.
- Krasnaya Kniga Rossiyskoy Federatsii. Zhivotnye [Red Book of the Russian Federation. Animals]. 2001. Ast and Astrel - Balashikha, Aginskoe - 862 p. (in Russian).
- Richardson W.J., Greene C.R., Malme C.I. and Thomson D.H. (1995). Marine mammals and noise. Academic Press Limited. 576 p.
- Sobolevsky Ye.I, et al. (Соболевский Е.И. и др.) (1999) Report for Sakhalin Energy Investment Company (Отчет для «Сахалин Энерджи Инвестмент Компани Лтд.»).
- Sobolevsky Ye.I, et al. (Соболевский Е.И. и др.) (2000) Report for Sakhalin Energy Investment Company (Отчет для «Сахалин Энерджи Инвестмент Компани Лтд.»).
- Yazvenko, S., T. MacDonald, S. Meier, S. Blokhin, S.R. Johnson, V. Vladimirov, S. Lagerev, M. Maminov, E. Razlivalov, M. Newcomer, R. Nielson, and V.C. Hawkes. 2002. Aerial marine mammal monitoring during the 2001 3-D seismic survey of the Odoptu block, northeast Sakhalin Island, Okhotsk Sea, Russia. Final Report by LGL Limited, Sidney, BC, for Exxon Neftegas Limited, Yuzhno-Sakhalinsk, Russia. 153 p. + Append.

Appendix A - Methodology for Normalizing and Analyzing the Acoustic Data

Normalizing and correcting the data was accomplished using the following algorithms³⁰:

1. Normalization of the raw data:

$$A = \frac{V}{K_g \cdot K_U} \quad [\mu\text{Pa}]$$

Where:

- A is the amplitude of the sample [μPa]
- V is the output voltage from the ADT
- K_U is the system gain
- K_g is the sensitivity of the hydrophone [$\text{mV}/\mu\text{Pa}$].

2. To calculate energy and power spectral density estimates:

For a digitized pressure time series:

$$p(i\Delta t) \quad , \quad i = 0, M-1 \quad [\mu\text{Pa}]$$

Where:

- M is the number of samples
- T is the length of the time series (seconds)
- Δt is the sample rate (seconds)

- A. Calculation of the energy spectral density within the analysis window T :

$$E(k\Delta f) = 2\Delta t^2 |P_{FFT}(k\Delta f)|^2 \quad [(\mu\text{Pa}/\text{Hz})^2] \text{ or } [\mu\text{Pa}^2 \cdot \text{s}/\text{Hz}]^{31}$$

Where:

$$\Delta f = \frac{1}{M\Delta t} \quad \text{is the frequency step (Hz)}$$

The FFT algorithm should be tested to ensure it satisfies Parsevals theorem:

³⁰ All programs for normalizing, correcting and averaging temporal and spectral data were tested. These tests used calibrated broadband and tonal signals transmitted from the hydrophone input to the output of the frequency discriminator of the radio-receiver, as well as the point where data from the ADT is input to the PC.

³¹ The factor of 2 compensates for the FFT being a 1-sided FFT ($k = 0, \dots, M/2$)

$$\sum_{i=0}^{M-1} p^2(i\Delta t)\Delta t = \sum_{k=0}^{M/2} E(k\Delta f)\Delta f$$

In order to satisfy Parseval's theorem there must be compensation by Δf otherwise the energies will not sum properly. In this way if the FFT is presented with a time window different than 1 second it will compensate for the window length³².

B. Calculation of the power spectral density (energy normalized to a 1 second window):

$$G(k\Delta f) = \frac{1}{T} E(k\Delta f) \quad [\mu\text{Pa}^2/(\text{s Hz})] \text{ or } [\mu\text{Pa}^2]$$

C. Conversion of the spectra to a logarithmic scale:

$$E_{dB}(k\Delta f) = 10\text{Log}2 + 20\text{Log}(\Delta t |P_{FFT}(k\Delta f)|) \quad [\text{dB re } 1 \mu\text{Pa/Hz}]^{33}$$

$$G_{dB}(k\Delta f) = E_{dB}(k\Delta f) - 10\text{Log}T \quad [\text{dB re } 1 \mu\text{Pa}^2/(\text{s Hz})]^{34}$$

D. Calculating average energy and power spectral density estimates over a window of length NT seconds by averaging spectra computed in consecutive non-overlapping windows of length T :

$$\bar{E}(k\Delta f) = \frac{2\Delta t^2}{N} \sum_{i=1}^N |P_{FFT}(k\Delta f)|^2 \quad [(\mu\text{Pa/Hz})^2] \text{ or } [\mu\text{Pa}^2 \cdot \text{s/Hz}]$$

$$\bar{G}(k\Delta f) = \frac{1}{T} \bar{E}(k\Delta f) \quad [\mu\text{Pa}^2/(\text{s Hz})] \text{ or } [\mu\text{Pa}^2]$$

$$\bar{G}(k\Delta f) = \frac{1}{N} \sum_{i=1}^N G(k\Delta f) \quad [\mu\text{Pa}^2/(\text{s Hz})] \text{ or } [\mu\text{Pa}^2]$$

Although the units for power spectral density are $\mu\text{Pa}^2/(\text{s Hz})$, $\mu\text{Pa}^2/\text{s/Hz}$ or μPa^2 , it is common usage to define the units for power spectral density as $\mu\text{Pa}^2/\text{Hz}$ or $\mu\text{Pa}/\sqrt{\text{Hz}}$.

³² For this calculation it is required that the FFT is scaled so that the output of a unit spike is unity at all frequencies. The scalar $S = \frac{1}{FFT(\delta(t))}$ should be applied to ensure correct scaling of the FFT.

³³ The window over which the energy estimate is calculated should be defined.

³⁴ The -10 log T correction allows power spectral density estimates to be calculated over longer windows for statistical stability.